

PETROLOGY AND MINERALOGY OF THE PCA 91082
CHONDRITE AND ITS COMPARISON WITH
THE YAMATO-793495 (CR) CHONDRITE

Takaaki NOGUCHI

*Department of Earth Sciences, Ibaraki University,
1-1, Bunkyo 2-chome, Mito 310*

Abstract: Petrographic and mineralogical study of the PCA 91082 CR chondrite was performed using a scanning electron microscope (SEM) and an electron microprobe analyzer (EPMA). The present study shows that this meteorite has some unique petrographic and mineralogical properties which have not been observed in other CR chondrites. (1) About 40% of chondrules contain silica-pods in their outermost parts. Silica was probably formed by the adhesion of SiO₂-rich materials during chondrule formation. (2) Chondrules in PCA 91082 experienced a lesser degree of aqueous alteration than those in other CR chondrites. Only the peripheries of chondrules are altered in PCA 91082. Fe contents in the phyllosilicates in chondrules are higher than the values reported in other CR chondrites in which chondrules are altered into their cores. In Yamato (Y)-793495, the extent of aqueous alteration is similar to that in PCA 91082. Fe contents of phyllosilicates in chondrules in Y-793495 are also higher than those in the more altered CR chondrites. (3) PCA 91082 contains constituent components which experienced various alteration conditions. One phyllosilicate clast in PCA 91082 contains a Ca-sulfate component with magnesian phyllosilicates. Probably the clast experienced aqueous alteration on a parent body. The aqueous alteration condition of the clast was probably similar to that of CIs.

1. Introduction

CR chondrites were first defined as a group of carbonaceous chondrites by McSWEEN (1979). Recently the CR chondrites have been established as a new chemical group due to the discovery of new samples from Antarctica and the Sahara desert (*e. g.* WEISBERG *et al.*, 1993; BISCHOFF *et al.*, 1993). Petrological, mineralogical, and chemical investigations of CR chondrites have revealed the properties of the this group. Their properties were summarized by WEISBERG *et al.* (1993). PCA 91082 is one of the most recently recognized CR chondrites (MASON, 1993). It was tentatively classified as a CR chondrite by MASON (1993), because the amount of matrix in this meteorite is much lower than in the other CR chondrites. I investigated the petrology and mineralogy of the PCA 91082 using a scanning electron microscope (SEM) and an electron microprobe analyzer (EPMA). The present study shows that this meteorite has some unique petrologic and mineralogical properties which have not been observed in other CR chondrites. The Yamato (Y)-793495 CR chondrite was also studied for comparison.

2. Samples and Methods

A polished thin section (PTS) of the PCA 91082,15 and a PTS of the Y-793495,91-1 were studied using an SEM and an EPMA. A detailed SEM observation was carried out with a JEOL JSM-840 equipped with an energy dispersive spectrometer (Link system). EPMA analysis was performed by a JEOL JXA-733 microprobe operated at 15 kV accelerating voltage and 9 nA beam current for silicates and oxides; and 15 kV and 20 nA for Fe-Ni metal. Bulk compositions of refractory inclusions, chondrules and matrix were analyzed by defocused beams ($\sim 40 \mu\text{m}$ in diameter for inclusions and chondrules, and $\sim 20 \mu\text{m}$ for matrix) at 15 kV and 9 nA. Correction by the BENCE and ALBEE (1968) method was used for the analyses of silicates, oxides, and bulk compositions of the inclusions, chondrules and matrix, and the ZAF method for Fe-Ni metal and sulfide. Special deconvolution programs were applied to correct for X-ray overlaps of K_{β} and K_{α} lines between some elements such as Ti and V, Ca and P, S and Co, and Co and Fe. Detection limits of EPMA analysis based on the BENCE and ALBEE correction for minor elements (wt%) were: SiO_2 , 0.08; TiO_2 , 0.08; Al_2O_3 , 0.07; Cr_2O_3 , 0.08; V_2O_3 , 0.07; FeO, 0.10; NiO, 0.13; MnO, 0.10; MgO, 0.07; ZnO, 0.20; CaO, 0.05; Na_2O , 0.06; K_2O , 0.05; P_2O_5 , 0.13; SO_3 , 0.04; Cl, 0.09.

The modal abundances of components (chondrules, matrix, etc.) were determined by point counting using transmitted light microscopy. Compositional mapping of some constituent components of this meteorite was performed by a JEOL JCM-733 mk II microprobe operated at 15 kV accelerating voltage and 120 nA. Counting time for each pixel (dwell time) was 40 ms.

3. Petrology and Mineralogy

3.1. General description

PCA 91082 is composed of chondrules, refractory-rich inclusions, mineral fragments, phyllosilicate clasts, dark inclusions, and matrix. Modal analysis of components of this meteorite shows that the matrix (+dark inclusions)/(chondrules+fragments) ratio is 0.49 (Table 1). This ratio is called here the matrix abundance. This value is lower than the values in the other CR chondrites, 0.59–1.85 (WEISBERG *et al.*, 1993). The true matrix abundance in PCA 91082 may be perhaps smaller than this value, because relatively large mineral and chondrule fragments (30–50 μm across) were included as matrix during point counting. This meteorite is highly weathered. Rust staining was observed in most chondrules. Metal particles in chondrules are weathered at their margins. The thickness of weathered metal margins is $< 3 \mu\text{m}$. Metal grains in the matrix are more weathered than those in chondrules. KALLEMEYN *et al.* (1994) reported that PCA 91082 shows a weak lineation; however, the PTS investigated in this study does not to show a lineation.

3.2. Refractory-rich inclusions

Refractory-rich inclusions are rare and much smaller than the chondrules, except for one Ca and Al-rich chondrule (1 mm across). They are 50–300 μm across. As in the other CR chondrites (*e.g.* WEISBERG and PRINZ, 1990; WEBER and BISCHOFF,

Table 1. Abundance (vol %) of components in the PCA 91082 and Renazzo.

	PCA 91082	Renazzo
Chondrules+chondrule fragments	66.7	54.0
Refractory inclusions	0.7	1.0
Matrix+dark inclusions	32.6	37.5
Number of points	2900	2000
Matrix (+DI) abundance	0.49	0.83

Modal abundance of the constituent components was determined by point counting using transmitted light microscopy. Data of Renazzo are from WEISBERG *et al.* (1993). Matrix (+DI) abundance was calculated by the equation (matrix+dark inclusions)/(chondrules+chondrule fragments).

1992), type A (or type A-like) inclusions are the most abundant. Compact type A inclusions in PCA 91082 have melilite cores with euhedral to subhedral spinel crystals (<5 μm in diameter) disperse in them, and are more abundant in the outer regions of the melilite cores. Tiny perovskite crystals (<2 μm across) are also included in the melilite cores. This inclusion has a Ca-pyroxene (diopside) rim (up to 10 μm thick). Fluffy type A-like inclusions were also found. They are aggregates of nodules which are composed of melilite cores rimmed by anorthite and diopside, and sometimes olivine. Euhedral to subhedral spinel is enclosed in melilite. Interstices of the objects are filled by matrix-like material. The texture of the fluffy type A-like inclusions is similar to that of the fluffy type A inclusions in Allende except for the presence of olivine in their rims (Fig. 1a) and the absence of secondary minerals such as nepheline and andradite (*e.g.* MACPHERSON *et al.*, 1988).

Amoeboid olivine inclusions were not observed in the PTS investigated. A few olivine-rich inclusions were observed. They contain abundant olivine and interstitial feldspathic materials. A Ca- and Al-rich chondrule (CAC) was observed. It is composed mainly of anorthitic plagioclase (>An_{98.8}), olivine, Ca-pyroxene (augite and pigeonite; Fig. 2), and a small amount of glass. Similar Ca- and Al-rich chondrules have been reported from a CR chondrite (WEISBERG and PRINZ, 1990) and CV chondrites and one ungrouped chondrite (plagioclase-olivine inclusions; SHENG *et al.*, 1991). But the CAC investigated is different from plagioclase-rich inclusions which contain Ti-Al-pyroxene and melilite (type C CAIs; WARK, 1987). A small amount of silica phase was observed in some areas in the interior of the CAC investigated (Fig. 1b). A CAC which contains a small amount of silica was observed in Coolidge (NOGUCHI, 1994). Different from the case of the CM chondrites (*e.g.* MACPHERSON *et al.*, 1988) these refractory-rich inclusions do not show evidence of aqueous alteration.

Table 2 shows some representative compositions of melilite, diopside, and spinel in the compact type A and fluffy type A-like inclusions. Melilite is gehlenite-rich ($\text{\AA}k_5\text{-}\text{\AA}k_{12}$). Similar gehlenite-rich melilite ($\sim\text{\AA}k_6$) was found in El Djouf 001 (WEISBERG, personal communication). The melilite is compositionally similar to that in the fluffy type A CAIs in Allende (*e.g.* MACPHERSON and GROSSMAN, 1984).

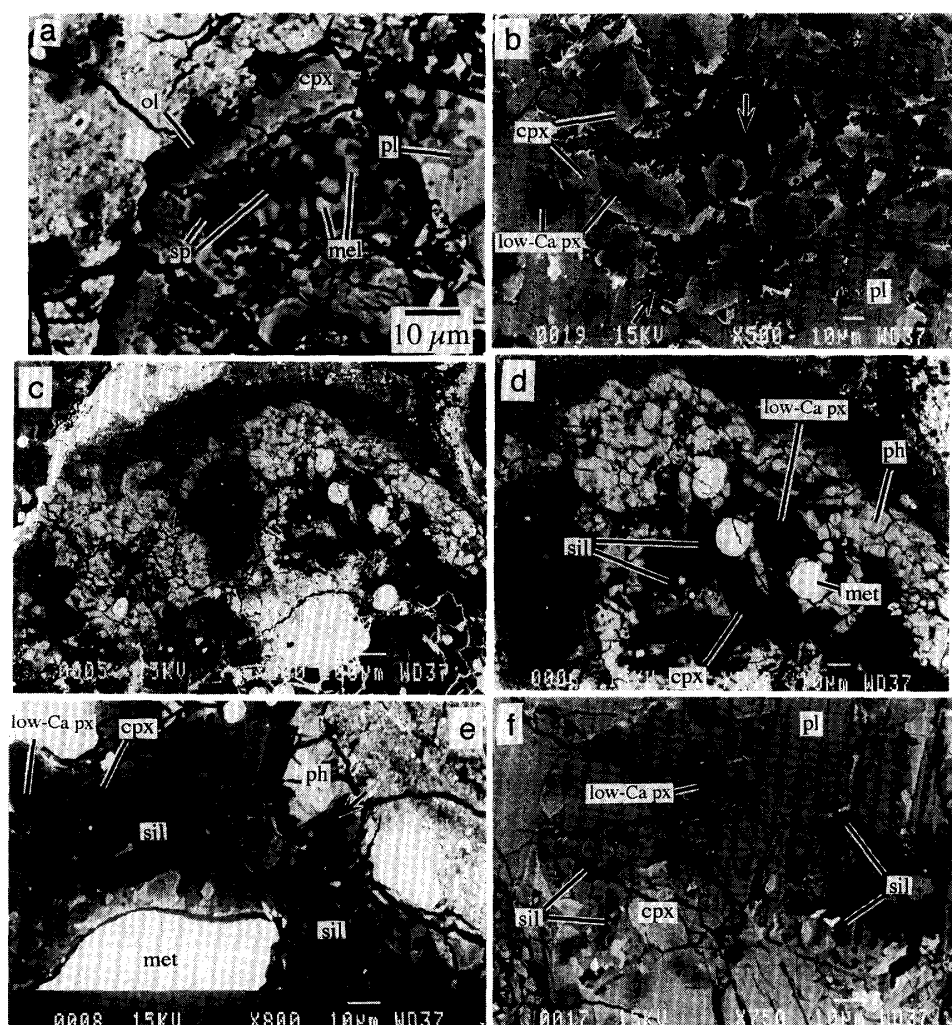


Fig. 1. Backscattered electron images (Figs. 1a-h, j-l) and a secondary electron image (Fig. 1i) of the PCA 91082 chondrite. (a) An enlarged image of a fluffy type A-like inclusion. This inclusion is composed of aggregates of nodules which are composed of melilite and spinel cores rimmed by anorthite (pl), diopside (cpx), and sometimes olivine (ol). Different from the fluffy type A inclusions in Allende, the rim of this inclusion contains olivine. (b) Interior of a Ca and Al-rich chondrule. This chondrule is composed mainly of plagioclase and Ca-pyroxene (augite). In some portions of this chondrule, aggregates of tiny silica (indicated by arrows) were observed. (c) A partially altered porphyritic olivine pyroxene (POP) chondrule. The outline of this chondrule is sinuous. Phyllosilicate (gray) is observed in the outermost part of the chondrule. The thickness of the phyllosilicate layer is $< 30 \mu\text{m}$. This irregularly-shaped chondrule has a fine-grained rim that fills depressions in the chondrule surface and renders the chondrule spherical. (d) An enlarged image of Fig. 1c. Silica exists as small dark pods. Their grain sizes are $< 5 \mu\text{m}$. Some pods are included in pyroxene. (e) The outermost part of a POP. Silica pods are also observed in this chondrule. They have elongated shapes and are larger than those in Fig. 1d. Mesostasis is indicated by an arrow. (f) The outermost part of a PO. Different from its interior, the outer zone of this chondrule is composed of euhedral plagioclase, pyroxene, and silica. The mineralogy of the chondrule core and rim indicates that the chondrule margin is more siliceous than the core.

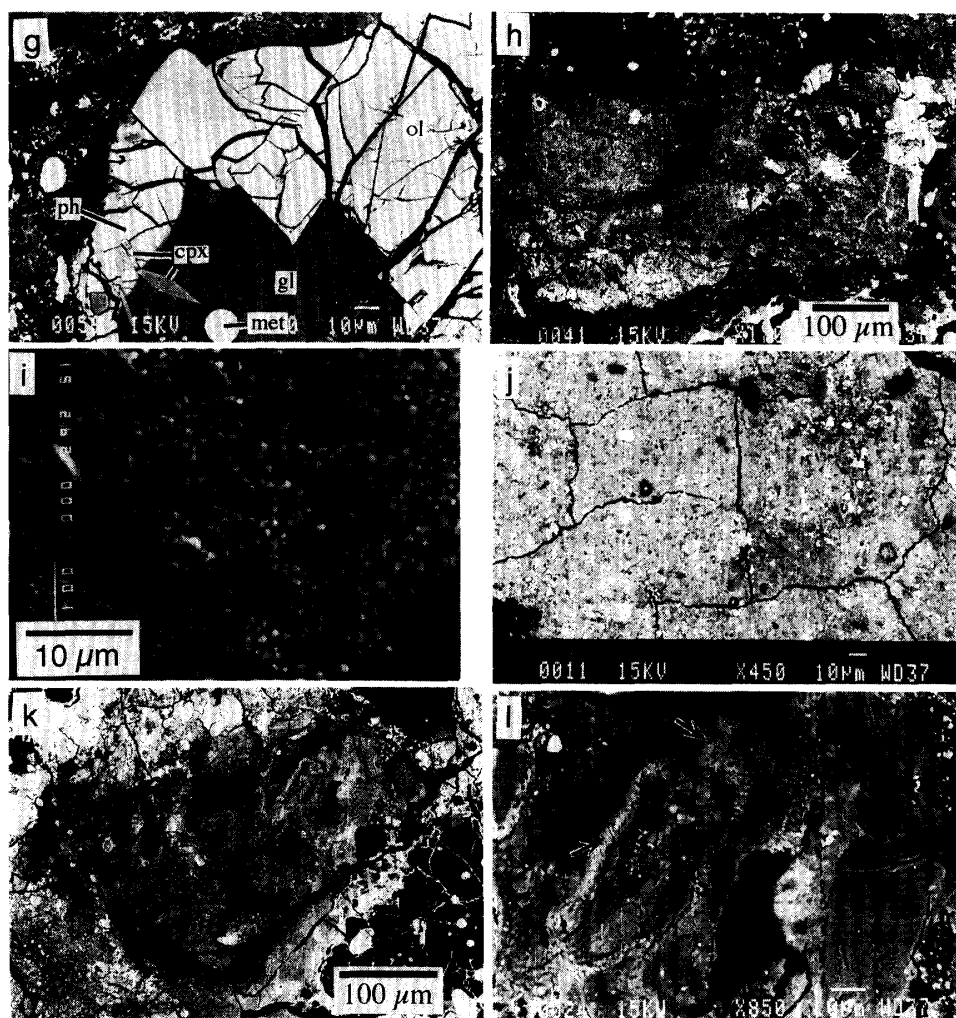


Fig. 1. (Continued)

(g) A type II porphyritic olivine (PO) chondrule. Chondrule glass which contacts the matrix shows alteration. The thickness of the phyllosilicate layer is $<40 \mu\text{m}$. (h) A dark inclusion. The outline of this dark inclusion is relatively sharp, but not all the outlines of dark inclusions are necessarily sharp. Magnesian low-Ca pyroxene fragments are rimmed by phyllosilicates (gray). Grain sizes of matrix minerals in this dark inclusion are coarser than the host matrix. Many ferroan olivine crystals ($<10 \mu\text{m}$ across) are observed. (i) A framboidal aggregate of magnetite. The framboidal aggregates occur in dark inclusions. They are formed by abundant fine-grained ($<1 \mu\text{m}$ across) and rare coarse ($<10 \mu\text{m}$ across) pure magnetite. (j) The matrix of this meteorite. Grain sizes of matrix materials are $<3 \mu\text{m}$ (most are sub- μm), except for mineral fragments. (k) A phyllosilicate clast. This clast is composed mainly of phyllosilicate. (l) An enlarged image of Fig. 1i. The clast is composed of coarse ($<30 \mu\text{m}$ across) and fine-grained (sub- μm) phyllosilicates. Ca and S are concentrated in a relatively bright area indicated by arrows. Abbreviations: mel, melilite; sp, spinel; pv, perovskite; low-Ca px, low-Ca pyroxene; cpx, Ca-pyroxene (diopside and augite); pl, plagioclase; ph, phyllosilicate; sil, silica phase; met, Fe-Ni metal; ol, olivine; gl, chondrule glass.

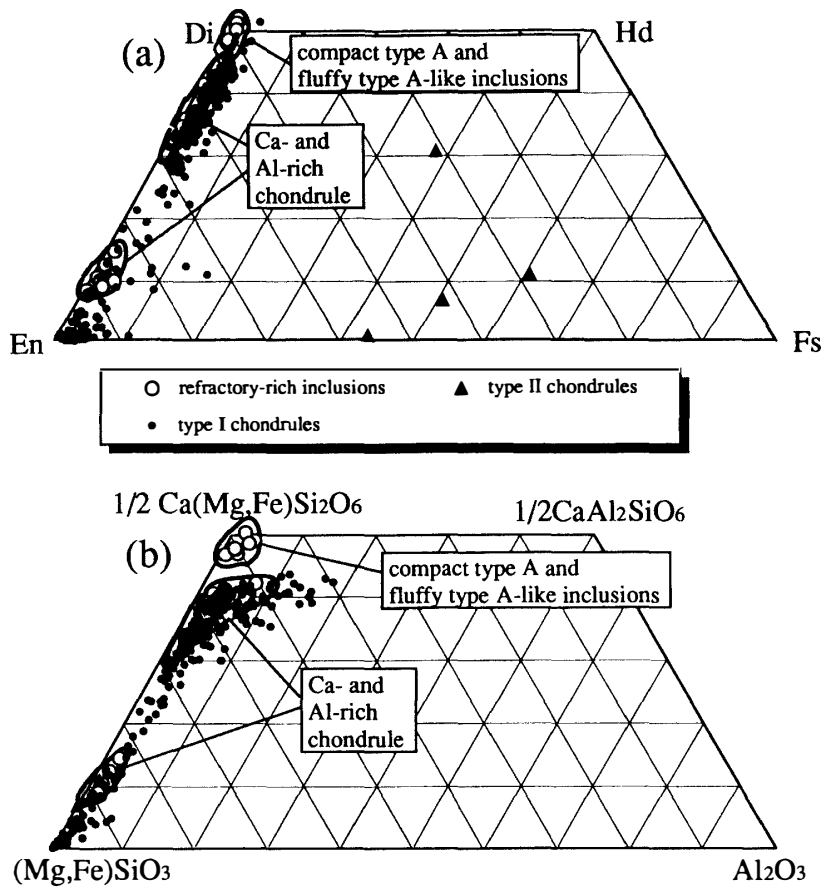


Fig. 2. A pyroxene quadrilateral diagram showing compositions of pyroxenes in refractory-rich inclusions, chondrules, and matrix in PCA 91082. Pyroxenes in chondrules are low-Ca clinopyroxene and augite. There is also pigeonite; primary orthopyroxene is rare. Chemical composition of Ca-pyroxene in type A and A-like inclusions is different from that in a Ca- and Al-rich chondrule (CAC). Ca-pyroxene in type A and A-like inclusions is diopside. On the other hand, Ca-pyroxene in a CAC is augite and has similar chemical composition to that in ferromagnesian chondrules.

Diopside in the CAIs contains <3.5 wt% Al_2O_3 (Fig. 3b). It is plotted near the $\text{Ca}(\text{Mg,Fe})\text{Si}_2\text{O}_6$ apex in the $\text{Wo}-(\text{En}+\text{Fs})-\text{Al}_2\text{O}_3$ diagram (Fig. 2b) because the concentration of the Ca-Tschermakite (CaTs) component is low. FeO, MnO and Cr_2O_3 concentrations in diopside in the CAIs are lower than those in chondrules. They are <0.5 , <0.2 , and <0.2 wt%, respectively. There is a compositional gap in Cr_2O_3 wt% between Ca-pyroxene in the type A and A-like inclusions and that in a CAC and ferromagnesian chondrules. The former contains <0.2 wt% Cr_2O_3 , the latter >0.5 . In the $\text{Wo}-(\text{En}+\text{Fs})-\text{Al}_2\text{O}_3$ diagram and the pyroxene quadrilateral diagram (Fig. 2), Ca-pyroxene in a CAC cannot be distinguished from pyroxene in ferromagnesian chondrules. In a plot of Al_2O_3 vs. TiO_2 wt% (Fig. 3b), it forms the trend which is different from a trend of Ca-pyroxene in ferromagnesian chondrules. The spinel contains <0.35 V_2O_3 wt% and <0.23 FeO wt% (Table 2). These values are consistent with the spinels in other CAIs (WEISBERG and PRINZ, 1990). Fa content of olivine in a fluffy type A-like inclusion and the CAC tends to be more magnesian

Table 2. Selected compositions of melilite, diopside, and spinel in the compact type A and fluffy type A-like inclusions.

Type of CAI mineral	Compact melilite	Fluffy melilite	Compact diopside	Fluffy diopside	Compact spinel	Fluffy spinel	Fluffy plagioclase
SiO ₂	24.26	24.09	53.15	54.63	bd	bd	42.17
TiO ₂	bd	bd	1.45	bd	0.12	bd	bd
Al ₂ O ₃	33.08	33.06	3.22	1.60	70.94	71.10	35.94
Cr ₂ O ₃	bd	bd	0.56	bd	bd	bd	bd
V ₂ O ₃	na	na	na	na	0.35	bd	na
FeO	bd	bd	0.26	bd	0.13	0.23	bd
MnO	bd	bd	0.11	bd	bd	bd	bd
MgO	1.79	1.49	20.04	17.58	29.13	28.13	bd
CaO	40.36	39.84	19.84	25.84	0.27*	0.08*	19.97
ZnO	na	na	na	na	bd	bd	na
Na ₂ O	bd	bd	0.14	bd	bd	bd	bd
Total	99.49	98.48	98.77	99.65	99.94	99.54	98.08

na: not analysed; bd: below detection.

*: These data are probably due to contamination from the surrounding melilite crystals because grain sizes of these spinels are small (slightly larger than 5 μm).

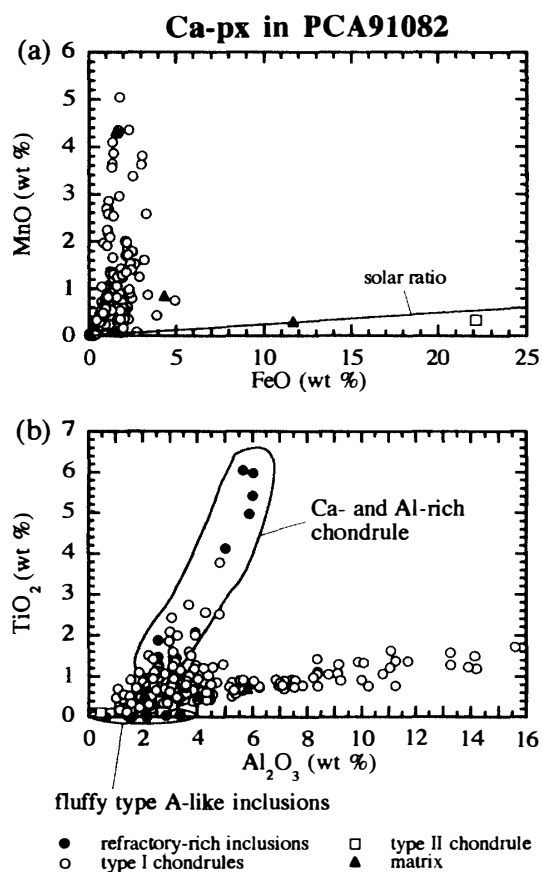


Fig. 3. Relationships between (a) FeO and MnO and (b) Al₂O₃ and TiO₂ in Ca-pyroxene in PCA 91082. FeO and MnO contents in Ca-pyroxene in type I chondrules are positively correlated. Al₂O₃ and TiO₂ contents in the Ca-pyroxenes are positively correlated. Two trends can be shown: one is for Ca-pyroxene in a CAC and some ferromagnesian chondrules and the other is for that in most of the ferromagnesian chondrules.

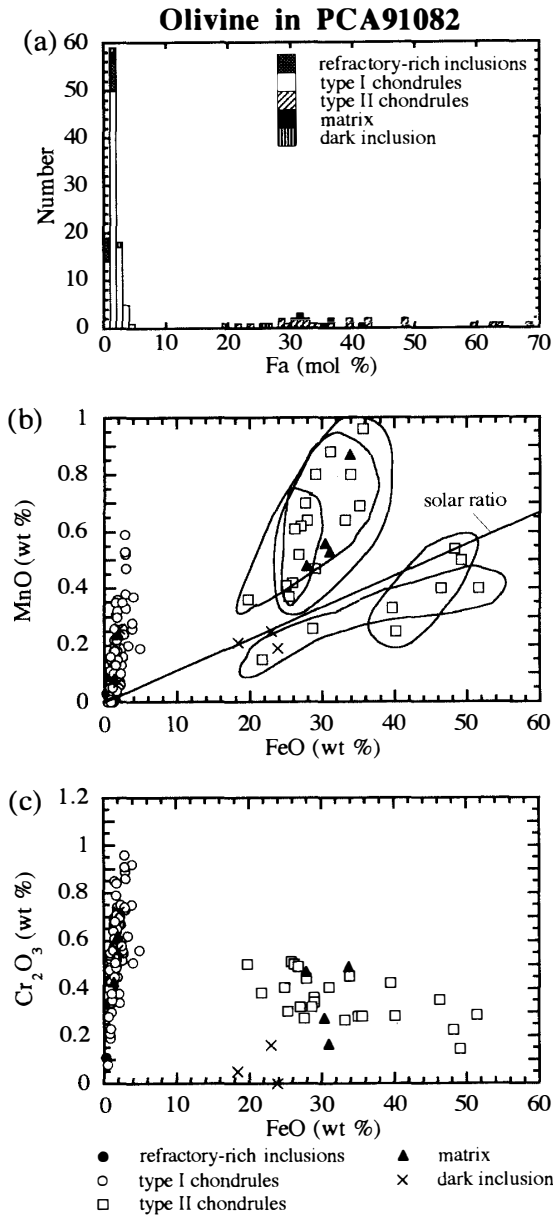


Fig. 4. Compositions of olivine in the PCA 91082. (a) A histogram of Fa mol %. Relationships between (b) FeO and MnO, and (c) FeO and Cr₂O₃. Figure 4a shows that olivine in type I chondrules has <Fa₅ (an average of Fa_{1.6}). Olivine in type II chondrules ranges from Fa₂₀ to Fa₇₀. There is a compositional gap between olivine in the type I and II chondrules. There are positive correlations between FeO and MnO, and between FeO and Cr₂O₃ contents, in olivine in type I chondrules. In Fig. 4b, olivine in each type II chondrule is enclosed by closed curves. There are two trends in Fig. 4b. In each trend, FeO and MnO wt% in olivine are positively correlated. Olivine in some type II chondrules and in a dark inclusion plots on or slightly below the line with the inclination of the solar Fe to Mn ratio. There is no obvious correlation (or there is a slightly negative correlation) between FeO and Cr₂O₃ concentrations in olivine in type II chondrules.

than that in the ferromagnesian chondrules (Fig. 4a). MnO concentration of the olivine in the refractory-rich inclusions is lower than that in most of the ferromagnesian chondrules (Fig. 4b).

3.3. Chondrules

3.3.1. General description

Ferromagnesian chondrules observed in this meteorite are porphyritic olivine (PO), porphyritic olivine pyroxene (POP), and barred olivine (BO) chondrules. BO chondrules are much rarer than porphyritic chondrules. Radial pyroxene and cryptocrystalline chondrules were not observed in the PTS investigated. The scarcity of chondrules other than porphyritic chondrules is common to other CR chondrites (e.g. WEISBERG *et al.*, 1993). The diameter of the largest chondrule is 1.9 mm. The

average diameter of 64 chondrules is 0.8 ± 0.4 (1σ) mm. WEISBERG *et al.* (1993) reported that the average diameter of CR chondrules is 0.8 mm. KALLEMEYN *et al.* (1994) also reported that the average chondrule diameter in CR chondrites, including PCA 91082, ranges from 490 to 770 μm . The average chondrule diameter is smaller than those in the CV chondrites (1 mm; GROSSMAN *et al.*, 1988).

Most of the PO and POP chondrules contain magnesian olivine ($< \text{Fa}_5$) and low-Ca pyroxene ($\text{Fs}_{1.6}$). The Fs content in low-Ca pyroxene is less than < 9 mol % (most are $< \text{Fs}_5$) (Fig. 2a). Chondrules containing these magnesian olivine and low-Ca pyroxene are type I chondrules. They usually contain Fe-Ni metal spherules in the chondrule margins. Abundant multilayered type I chondrules are common to other CR chondrites (WEISBERG *et al.*, 1993; BISCHOFF *et al.*, 1993). In the porphyritic chondrules, calcic plagioclase and Ca-pyroxene (augite) are often observed in addition to olivine and low-Ca pyroxene. Aluminous spinel was not observed in the ferromagnesian chondrules. Olivine phenocrysts concentrate in the chondrule cores and low-Ca pyroxene phenocrysts occupy the chondrule margins. Devitrified brown glass and in some cases clear glass were observed in the interior of the chondrules. Therefore, the extent of aqueous alteration in these chondrules is relatively low. The outermost parts of the chondrules are usually composed of relatively small grains (< 30 μm across) of low-Ca pyroxene, augite, \pm plagioclase, \pm silica, \pm olivine, \pm chondrule glass, and phyllosilicates. Olivine is rare in the chondrule margins and there was no olivine crystal which contacts silica. Silica-bearing chondrules will be described later.

Phyllosilicates were observed within only 20–50 μm from the chondrule margins (Fig. 1c). Under an optical microscope, many chondrule margins are brown, as is common to other CR chondrites (WEISBERG *et al.*, 1993). The occurrences of phyllosilicates in magnesian chondrules suggests that the phyllosilicates replace mainly chondrule glass, and low-Ca pyroxene, plagioclase, and Fe-Ni metal spherules are also replaced (*e.g.* Fig. 1d). The sinuous outline is a common feature of chondrules in PCA 91082 (Fig. 1c). In some cases, these irregular-shaped chondrules have fine-grained rims that fill depressions in the chondrule surface and render the chondrule spherical (Fig. 1c). The fine-grained rims are probably composed mainly of serpentine because compositions of the rims are similar to those of the matrix.

3.3.2. Silica-bearing chondrules

It is interesting that some pod-like objects are observed near the outer Fe-Ni metal rich zones in layered chondrules. Figures 1d and e show enlarged images of the outermost parts of type I chondrules. Such pod-like objects are up to 10 μm in diameter. They are mainly composed of SiO_2 (96.14–99.14 wt%) and contain minor amounts of Al_2O_3 (0.24–0.59 wt%), FeO (0.46–1.27 wt%), MgO (< 0.07 –0.48 wt%), CaO (< 0.05 –0.17 wt%), and Na_2O (< 0.06 –0.23 wt%). Figure 1f shows the outer zone of a PO chondrule which is composed of euhedral plagioclase, pyroxene, silica, and mesostasis. It is not clear whether these pods are crystallites or amorphous material, although their morphology (Fig. 1f) suggests that some are tridymite. WEISBERG *et al.* (1993) observed chondrule rims of other CR chondrites in details by SEM; however, no silica-pods were reported.

Chondrules which include SiO_2 pods and almost FeO-free ferromagnesian silicates have also been reported from Murchison CM2 chondrite (OLSEN, 1983).

OLSEN (1983) observed two such chondrules among 20 chondrules investigated. In PCA 91082, however, 28 chondrules contain such silica pods among the 64 chondrules investigated. Mineral species are almost the same between silica-bearing chondrules in Murchison and those in PCA 91082, but their relative abundances are different. Chondrules containing silica pods in Murchison contain Fe-Ni metal in their cores, and do not have a layered structure. The two chondrules in Murchison have SiO₂-rich compositions (>50 wt%). On the other hand, in the two chondrules in PCA 91082, the chondrule cores contain abundant olivine phenocrysts and seldom have silica pods. The chondrule cores in the silica pod-bearing chondrules are almost identical to the those in the silica-free chondrules in terms of mineralogy and chemistry. This means that in silica-bearing chondrules only the chondrule margins contain higher SiO₂ content and not the chondrule cores. Thicknesses of the chondrule margins vary and are generally thin (<70 μm). Therefore, bulk compositions of the silica-bearing chondrules overlap those of silica-free chondrules (Fig. 12).

3.3.3. Type II chondrules

There are some PO and BO chondrules including ferroan olivine, and small amounts of ferroan augite, ferroan low-Ca pyroxene, chromite (Y_{Cr} : 0.91~0.99; TiO₂: 0.83~1.26 wt%; V₂O₃: 0.57~0.93 wt%; ZnO: not detected), Fe-Ni metal and chondrule glass. Olivine in the ferroan chondrules shows compositional zoning. For example, in a ferroan PO, olivine phenocrysts show zoning from Fa₂₄ to Fa₆₉. Relic magnesian core was not observed in ferroan olivine phenocrysts. Chondrules containing ferroan olivine (>Fa₂₀) are called here type II chondrules. Phyllosilicates are observed where chondrule glass contacts to the matrix (Fig. 1g). Because the amount of chondrule glass is higher than that of most of the magnesian chondrules, the reaction front of the altered zone can be clearly shown (Fig. 1g). The thickness of the phyllosilicate layer is <40 μm.

3.3.4. Composition of olivine, pyroxene, and Fe-Ni metal

A histogram of Fa content shows that olivine in type I chondrules have less than 5 mol % (Fig. 4a), and an average of Fa_{1.6}. This value is consistent with the data from other CR chondrites (*e.g.* WEISBERG *et al.*, 1993). Olivine in type II chondrules ranges from Fa₂₀ to Fa₇₀ (Fig. 4a). There is a compositional gap between olivines in type I and II chondrules.

There are positive correlations between FeO and MnO, and between FeO and Cr₂O₃ contents in olivine in type I chondrules (Fig. 4b and c). Olivine in type II chondrules shows tow trends (Fig. 4b). In each trend, FeO and MnO concentrations in olivine in type II chondrules are positively correlated. There is no obvious correlation (or slightly negative correlation) between FeO and Cr₂O₃ concentrations in olivine in type II chondrules (Fig. 4c). CaO content in olivine in type I and II chondrules is >0.05 wt%. Selected data of olivine in type I and II chondrules are shown in Table 3.

Pyroxenes in type I chondrules are low-Ca clinopyroxene and augite. Figure 2a suggests that there is also pigeonite and that primary orthopyroxene is rare. Low-Ca pyroxene in type II chondrules contains >Fs_{43.2}. Although augite is often observed in type II chondrules, only one good analysis was acquired (Fs_{37.8}) due to the small grain size (<5 μm). In the Wo-(En+Fs)-Al₂O₃ diagram (Fig. 2b), pyroxenes in type I and II chondrules are plotted in the same area.

Table 3. Selected compositions of olivine, low-Ca pyroxene, Ca-rich pyroxene, and plagioclase in chondrules.

Chondrule mineral	Type I olivine	Type II olivine	Type I low-Ca px	Type I Ca-rich px	Type I plag*
SiO ₂	42.28	35.69	58.70	54.16	43.98
TiO ₂	bd	bd	0.08	0.87	bd
Al ₂ O ₃	bd	bd	0.68	2.01	34.88
Cr ₂ O ₃	0.57	0.28	0.95	0.74	bd
FeO	1.65	35.65	1.62	1.57	bd
MnO	bd	0.96	0.18	0.46	bd
MgO	55.08	27.07	37.25	20.79	0.51
CaO	0.22	0.26	0.41	19.32	19.95
Na ₂ O	bd	bd	bd	0.06	0.23
Total	99.80	99.91	99.87	99.98	99.55

bd: below detection.

#: Stoichiometry of plagioclase in chondrules in this meteorite is not good, and MgO is always detected in a small amount.

Relationships between FeO and MnO, FeO and Cr₂O₃, and Al₂O₃ and TiO₂ in low-Ca pyroxene are similar to those in augite. FeO and MnO contents in low-Ca pyroxene in type I chondrules is positively correlated (Fig. 5) as is the case of olivine in the same chondrules (Fig. 4b). Low-Ca pyroxene in type II chondrules plots along a line with inclination of the solar Fe to Mn ratio. Cr₂O₃ concentrations in pyroxenes are >0.5 wt%. Different from the case of olivine, the correlation between FeO and Cr₂O₃ in the pyroxenes is not clear. Al₂O₃ and TiO₂ contents in the pyroxenes are positively correlated. As described previously, Ca-pyroxene shows two trends (Fig. 3b). Some Ca-pyroxenes in type I chondrules are plotted in the area where pyroxenes in a CAC are plotted: The similar two trends are shown in Ca pyroxenes in chondrules in the Allende CV3 chondrite (NOGUCHI, 1989). Selected analyses of pyroxenes in type I chondrules are shown in Table 3.

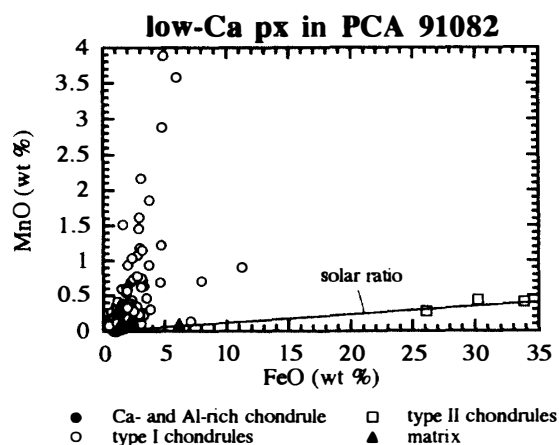


Fig. 5. Relationships between FeO and MnO in low-Ca pyroxene in PCA 91082. FeO and MnO contents in low-Ca pyroxene in type I chondrules are positively correlated. Low-Ca pyroxene in type II chondrules plots along a line with the inclination of the solar Fe to Mn ratio. The low-Ca pyroxene coexists with olivine, which is plotted slightly below the line with the inclination of the solar Fe to Mn ratio in Fig. 4b.

Type I chondrules often contain plagioclase as laths and sometimes microphenocrysts (Fig. 1f). Microprobe data of such plagioclase crystals usually contain MgO (average 0.85 wt%) and FeO (average 0.33 wt%) (Table 3). Preliminary TEM observation shows that the crystallinity of such plagioclase is good. However, sub- μm sized precipitates which were reported from plagioclase in CAIs in Allende (BARBER *et al.*, 1984) have not been found yet.

Many metal grains in chondrules are kamacite (Fig. 6). Taenite was not observed in the PTS investigated. Fe-bearing sulfides in this meteorite are troilite or pyrrhotite and pentlandite. Figure 6 shows the relationships between Ni and minor elements (Co, Cr, and P). Compositional range of Ni, Co, Cr, P contents are 4.1–17.0, 0.14–0.61, below detection–1.29 wt%, and below detection–0.75, respectively. Ni and Co contents of Fe-Ni metal in the peripheries of chondrules are lower than those in the cores of chondrules (Fig. 6a). There is a positive correlation between these elements with a solar Ni:Co ratio. These data are consistent with those of WEISBERG *et al.* (1988, 1993) and LEE *et al.* (1992).

3.3.5. Composition of phyllosilicates in chondrules

Figure 7 and Table 4 show chemical compositions of phyllosilicates in chondrules in PCA 91082. The (Si+Al)-Mg-Fe and (Mg+Fe)-Al-Si diagrams indicate that most

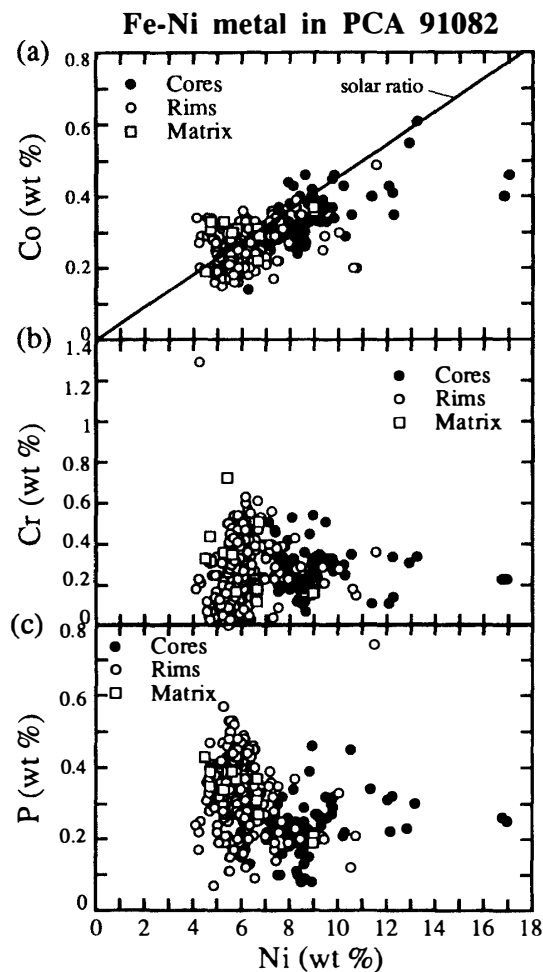


Fig. 6. Relationships between (a) Ni and Co, (b) Ni and Cr, and (c) Ni and P, in Fe-Ni metal in PCA 91082. Ni and Co contents of Fe-Ni metal in the chondrule margins are lower than those in the cores of chondrules. There is a positive correlation between these elements with the solar Ni:Co ratio. These data are consistent with those from other CR chondrites (WEISBERG *et al.*, 1988, 1993; LEE *et al.*, 1992).

of the phyllosilicates in type I chondrules are the mixtures of serpentine, Al-rich serpentine (or chlorite) and smectite. The proportion of each phase probably depends on the bulk compositions of the altered materials (in other words, the proportions of low-Ca pyroxene, plagioclase, chondrule glass, and Fe-Ni metal). The phyllosilicates in type II chondrules have more restricted compositions than those in type I chondrules (Fig. 7). The Fe/(Mg+Fe) ratios in the phyllosilicates in type II

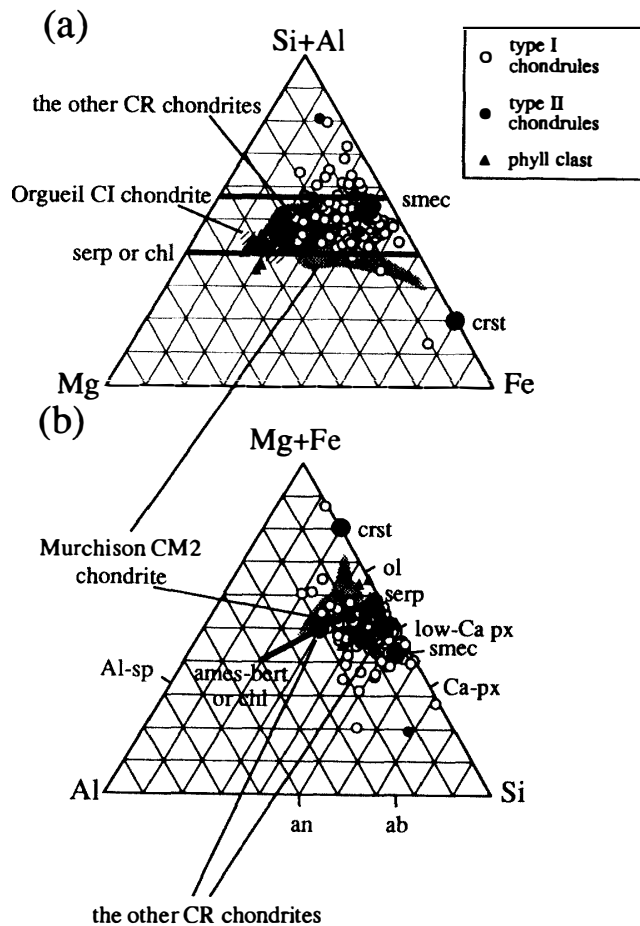


Fig. 7. Chemical compositions of phyllosilicates in chondrules and a phyllosilicate clast in PCA 91082. (a) A (Si+Al)-Mg-Fe diagram. (b) A (Mg+Fe)-Al-Si diagram. Compositions of phyllosilicates in chondrules in Murchison CM2 chondrite (NOGUCHI, unpublished data) and in the other CR chondrites (WEISBERG et al., 1993), and in the Orgueil CI chondrite (TOMEOKA and BUSECK, 1988). Compositions of some minerals are also indicated. These diagrams are plotted based on atomic ratios in this paper. These diagrams indicate that most of the phyllosilicates in type I chondrules are the mixtures of serpentine, Al-rich serpentine (or chlorite) and smectite. The phyllosilicates in type II chondrules have more restricted compositions than those in type I chondrules. The phyllosilicates in type II chondrules are the mixtures of Al-rich serpentine or chlorite and smectite (Fig. 7b). The Fe/(Mg+Fe) ratio of the phyllosilicates in PCA 91082 is higher than that in other CR chondrites. Abbreviations: serp, serpentine; chl, chlorite; smec, smectite; crst, cronstedtite; ames, amesite; bert, berthierine; Al-sp, aluminous spinel; an, anorthite; ab, albite; Ca-px, Ca-pyroxene; low-Ca px, low-Ca pyroxene; ol, olivine.

Table 4. Selected compositions of phyllosilicates in chondrule margins.

Chondrule	Type I	Type I	Type II
SiO ₂	40.19	37.32	33.32
TiO ₂	bd	bd	0.12
Al ₂ O ₃	1.00	1.29	7.47
Cr ₂ O ₃	bd	bd	bd
FeO	35.96	35.67	35.43
NiO	bd	bd	bd
MnO	0.60	0.19	0.11
MgO	2.38	5.65	4.57
CaO	0.20	0.06	bd
Na ₂ O	1.86	1.30	1.51
K ₂ O	0.40	0.22	0.41
P ₂ O ₅	bd	bd	0.36
SO ₃	0.30	0.34	0.54
Total	82.89	82.04	83.84

bd: below detection.

chondrules are as high as the highest Fe/(Mg+Fe) ratios in the phyllosilicates in type I chondrules (Fig. 7a). The phyllosilicates in type II chondrules are the mixtures of Al-rich serpentine or chlorite and smectite (Fig. 7b).

Figure 8 shows the relationships between the compositions of chondrule glass, plagioclase, and phyllosilicates in type I and II chondrules. The distinctions between unaltered chondrule glass, weakly altered chondrule glass, and phyllosilicates are based only on the total wt%; the boundaries are 97 and 90 wt%, respectively. Because various amounts of fine crystals, such as plagioclase, are often observed as relicts in weakly altered glass, the compositions of the weakly altered chondrule glass overlap with those of unaltered chondrule glass, and rarely with phyllosilicates (Fig. 8). In Fig. 8, the weakly altered chondrule glass is plotted in two regions; one is the same region of chondrule glass and another region is situated among the regions of plagioclase, chondrule glass, and phyllosilicates. The data suggest that the weakly altered chondrule glass is composed of the phyllosilicates and relict plagioclase and glass. In type II chondrules, there are reaction fronts in chondrule glass as shown in Fig. 1g. A compositional gap between unaltered and weakly altered chondrule glass and phyllosilicates corresponds to the compositional change at the reaction fronts.

WEISBERG and PRINZ (1991a, b) and WEISBERG *et al.* (1993) reported on the phyllosilicates in the chondrules in Al Rais, Renazzo, and Y-790112. In Al Rais and Renazzo, many chondrules are altered into their cores. Phyllosilicates in their chondrule cores are optically greenish to light brown and Al-rich (10–15 wt% Al₂O₃). These data suggest that they are the mixtures of chlorite and smectite. Chondrule rims are optically green to light brown and compositionally the mixtures of Fe-rich serpentine and smectite. Like the Algerian and other Antarctic CR chondrites (WEISBERG and PRINZ, 1991a, b; WEISBERG *et al.*, 1993; BISCHOFF *et al.*, 1993),

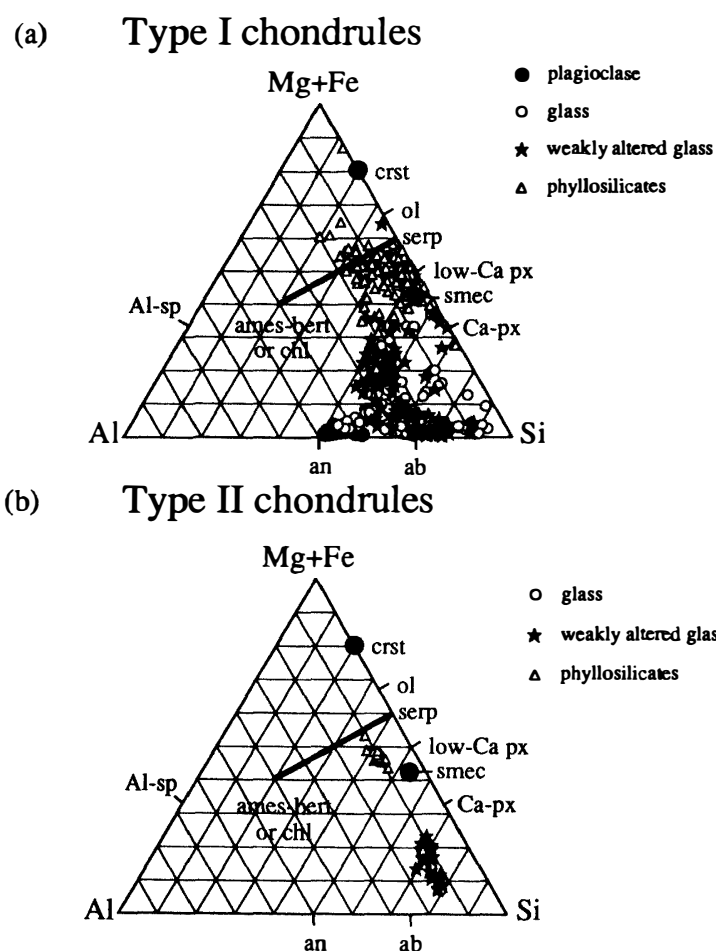


Fig. 8. Comparison of chemical compositions of plagioclase, chondrule glass, weakly altered chondrule glass, and chondrule phyllosilicates in type I and type II chondrules in PCA 91082. These diagrams are plotted based on atomic ratios in this paper. The boundaries between unaltered chondrule glass, weakly altered chondrule glass, and phyllosilicates are determined based only on the total wt%; the boundaries are 97 and 90 wt%, respectively. Because various amounts of fine crystals, such as plagioclase and Ca-pyroxene, are often observed as relicts in weakly altered glass, the compositions of the weakly altered chondrule glass overlap with those of unaltered chondrule glass, and rarely with phyllosilicates. The phyllosilicates in type II chondrules have more restricted compositions than those in type I chondrules. A compositional gap between the unaltered and weakly altered chondrule glass and phyllosilicates corresponds to the compositional change at the reaction fronts. Abbreviations are the same as those in Fig. 7.

phyllosilicates are observed in the chondrule margins in PCA 91082. However, the compositions of the phyllosilicates in PCA 91082 are different from the phyllosilicates in the outer layers of chondrules in Y-790112 as well as Al Rais and Renazzo (Fig. 7). It is clear that Fe contents of the phyllosilicates in PCA 91082 are higher than those in the three CR chondrites. In Fig. 7, EPMA analyses of the phyllosilicates in chondrules in Murchison CM2 chondrite are also plotted (NOGUCHI, unpublished data). The phyllosilicates in chondrules in Murchison are plotted in different areas from those in PCA 91082 and the other CR chondrites. The data suggest that

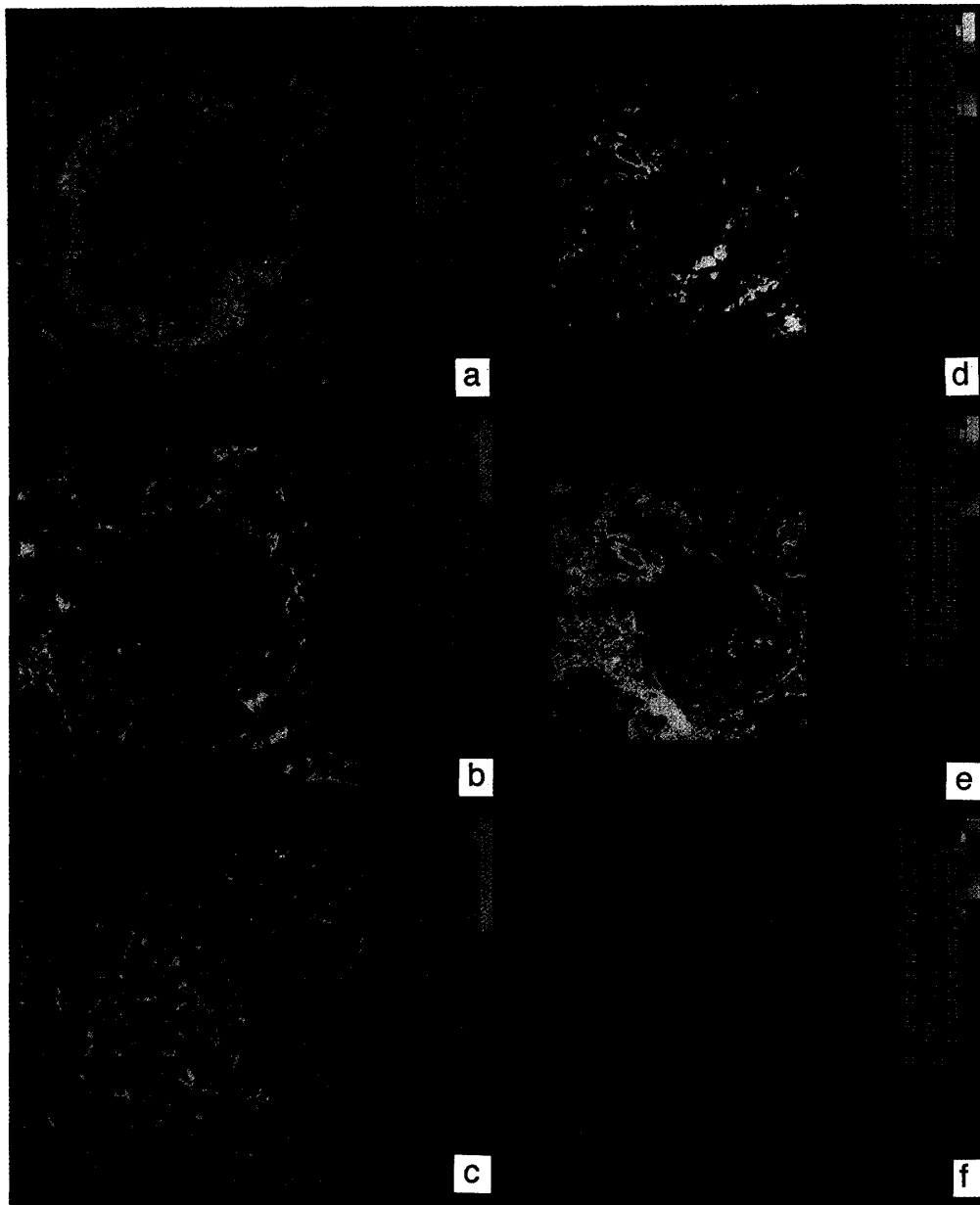


Fig. 9. Compositional mapping of a POP chondrule and a phyllosilicate clast in PCA 91082. (a)~(c) Intensity maps of a POP: (a) Mg K_{α} line, (b) Na K_{α} line, and (c) Ca K_{α} line. (d)~(f) Intensity maps of a phyllosilicate clast: (d) Ca K_{α} line, (e) S K_{α} line, and (f) Fe K_{α} line. Ca and Na concentrations in chondrule glass varies from the chondrule core to the chondrule margin in this PO chondrule. Ca concentration decreases and Na concentration increases from the core to the margin. The large decrease and increase of these elements are shown where the mode of olivine (Mg-rich grains in Fig. 9a) decreases and most of the Fe-Ni metal spherules (black grains in Fig. 9a) are situated (compare Fig. 9b and c with Fig. 9a). Such compositional zoning of chondrule glass can be seen in both silica-bearing or silica-free type I chondrules. Intensity maps of the phyllosilicate clast show that where both Ca and S are concentrated, Fe is depleted (Fig. 9d-f). Ca and S enriched areas appear sporadically in the clast. The largest Ca and S enriched area is indicated by arrows in Fig. 11. The shapes and occurrences of the Ca and S enriched areas suggest that they are perhaps heavily altered Ca-rich pyroxene rims on low-Ca pyroxene.

constituent phyllosilicates are different between CR and CM chondrites. TEM observation and AEM analysis of the phyllosilicates in chondrules in Murchison (NOGUCHI *et al.*, 1993) and Y-791198 (AKAI and KANNO, 1986) show that the phyllosilicates in chondrules in CM chondrites are mixtures of cronstedtite and berthierine or chlorite. In CM chondrites, chondrule phyllosilicates with similar compositions to those in CR chondrites occur only in a small amount on a sub- μm scale (NOGUCHI *et al.*, 1993). Alkaline element concentration in the phyllosilicates in chondrules in PCA 91082 is higher than that in other CR chondrites. This problem will be discussed later.

3.3.6. Compositional zoning of chondrule glass in type I chondrules

Ca and Na concentrations in chondrule glass varies from the chondrule cores to the chondrule margins in PO and POP chondrules (Fig. 9c and d). Ca concentration decreases and Na concentration increases from the cores to rims. In some cases, K concentration increases as well as Na at the chondrule margins. Large decrease and increase of these elements are shown where the mode of olivine (Mg-rich grains in Fig. 9a) decreases and most of the Fe-Ni metal spherules (black grains in Fig. 9a) are situated (Compare Fig. 9b and c with Fig. 9a). Such compositional zoning of chondrule glass can be seen in both silica-bearing or silica-free type I chondrules. However, these conspicuous compositional changes in chondrule glass were not observed in each type II chondrule. Major element compositions of chondrule glass in type II chondrules are more homogeneous than those in type I chondrules (Fig. 8). The conspicuous compositional variation of chondrule glass within each type I chondrule is one of the unique petrographic properties of this meteorite. For example, most chondrule glass in Y-793495 does not show such definite compositional change within each chondrule. The compositional variation of fresh and weakly altered chondrule glass in Y-793495 is smaller than that in PCA 91082.

3.4. Dark inclusions

CR chondrites contain dark inclusions (*e.g.* WEISBERG *et al.*, 1993; BISCHOFF *et al.*, 1993; ENDREß *et al.*, 1994). PCA 91082 also contains some dark inclusions. Their sizes are less than 600 μm across. Different from the case of Acfer 059 and El Djouf 001 (BISCHOFF *et al.*, 1993; ENDREß *et al.*, 1992, 1994), the boundaries between dark inclusions and matrix are not always sharp. Dark inclusions are optically opaque to dark brown. They are composed of fine-grained silicates (anhydrous and hydrous ones), opaque minerals (magnetite and sulfides), and Ca-carbonate. The proportions of these minerals vary among dark inclusions. These observations are consistent with the previous studies (*e.g.* WEISBERG *et al.*, 1993; BISCHOFF *et al.*, 1993; ENDREß *et al.*, 1994).

Although petrographic features of the dark inclusions are basically similar to those of the matrix, there are also some petrographic differences between the dark inclusions and the matrix. Figure 1h shows a dark inclusions in this meteorite. The extent of aqueous alteration shown in this dark inclusion seems to be higher than that in the matrix. Replacement of low-pyroxene fragments by phyllosilicates is more obvious than that in matrix (Fig. 1h). Grain sizes of matrix minerals of this dark inclusion are larger than in the host matrix. The matrix of the inclusion contains not only magnesian olivine fragments whose compositions are very similar to those in

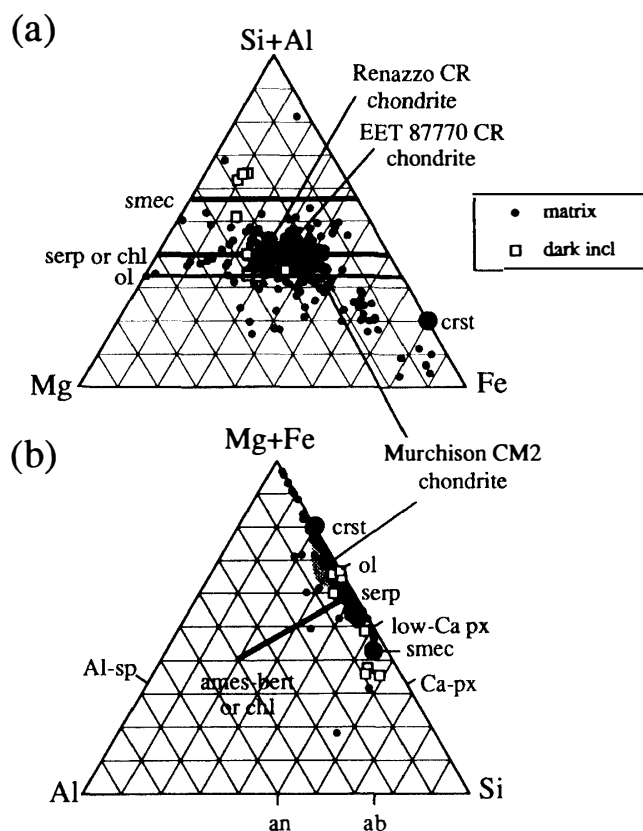


Fig. 10. Chemical compositions of the matrix in PCA 91082. (a) A (Si+Al)-Mg-Fe diagram. (b) A (Mg+Fe)-Al-Si diagram. Compositions of the matrix in Murchison CM2 chondrite (NOGUCHI, unpublished data), the matrix average compositions in Renazzo and EET 87770 (ZOLENSKY *et al.*, 1993), and compositions of some minerals are also indicated. These diagrams are plotted based on the atomic ratios in this paper. This figure suggests that fine-grained ($< 3 \mu\text{m}$ across) materials of the matrix are mainly composed of olivine, serpentine, smectite, and Fe-bearing phase(s) (Fe-Ni metal, magnetite, and sulfides). The average composition of the Renazzo matrix has a slightly higher (Si+Al)/(Si+Al+Mg+Fe) ratio than most of the ratios of the PCA 91082 matrix. The average composition of EET 87770 (ZOLENSKY *et al.*, 1993) has a similar (Si+Al)/(Si+Al+Mg+Fe) ratio to the ratios of the PCA 91082 matrix. Abbreviations are the same as those in Fig. 7.

type I chondrules but also many fine-grained ($< 10 \mu\text{m}$ across) ferroan olivine crystals (Fa₂₅-Fa₃₀). Figure 4b shows that their FeO to MnO ratios are near the solar ratio. Cr₂O₃ and CaO concentrations of these olivine crystals (< 0.08 – 0.16 and < 0.05 – 0.04 wt%, respectively) are lower than the olivine with similar FeO concentration in type II chondrules (0.16 – 0.62 and 0.17 – 0.48 , respectively). The ferroan olivines in the dark inclusion were perhaps not derived from type II chondrules. Figure 10 suggests that this dark inclusion contains ferroan olivine and augite, and that the phyllosilicate content is low. The Fe/(Mg+Fe) ratio of the olivine component is around 0.45 (Fig. 10a), higher than that in the ferroan olivine with 5–10 μm in diameter. These data suggest that finer olivine is more ferroan than coarser olivine. In the matrix of a dark

inclusion, some data show that Ca and S are positively correlated. The texture where Ca and S show a positive correlation is not different from that of the surroundings. Perhaps the carrier phase of Ca and S is very fine (sub- μm) and dispersed. It is different from the case of a phyllosilicate clast which will be described later.

Aggregates of framboidal magnetite are shown in the dark inclusions (Fig. 1i). In some dark inclusions, they are much more abundant than in others. Magnetite in dark inclusions is almost pure Fe_3O_4 . The NiO concentration of magnetite from a framboidal aggregate is <0.15 wt%. Its MnO, MgO, and Cr_2O_3 concentrations are below the detection limits. This is consistent with ENDREß *et al.* (1994).

3.5. Matrix

The matrix appears opaque under an optical microscope. The matrix of PCA 91082 is composed of fine-grained (sub- μm) olivine, pyroxene, and phyllosilicates, and opaque minerals (Fe-Ni metal and sulfides) (Fig. 1j). Except for the silicate mineral fragments, most of the fine-grained mineral grains in the matrix are too fine to be identified by SEM and EPMA.

Chemical compositions of olivine, low-Ca pyroxene, and Ca-rich fragments in the matrix show that most of them are similar to the compositions of these minerals in both type I and II chondrules (Figs. 3, 4, and 5). Many Fe-Ni metal grains in the matrix are highly altered. Fe-Ni metal in the matrix also has similar composition to that in chondrules (Fig. 6). Therefore, most of these minerals were probably derived from chondrules.

Figure 10 suggests that fine-grained (<3 μm across) materials of the matrix are mainly composed of olivine, serpentine, smectite, and Fe-bearing phase(s) (for example, Fe-Ni metal, magnetite, and sulfides). The average composition of the Renazzo matrix (ZOLENSKY *et al.*, 1993) has slightly higher $(\text{Si} + \text{Al})/(\text{Si} + \text{Al} + \text{Mg} + \text{Fe})$ ratio than most of the ratios of the PCA 91082 matrix. The average composition of EET 87770 (ZOLENSKY *et al.*, 1993) has a similar $(\text{Si} + \text{Al})/(\text{Si} + \text{Al} + \text{Mg} + \text{Fe})$ ratio to the ratios of the PCA 91082 matrix. TEM studies of the matrices of CR chondrites show that they are composed of olivine, saponite, and serpentine (ZOLENSKY, 1991; ZOLENSKY *et al.*, 1993). The lower $(\text{Si} + \text{Al})/(\text{Si} + \text{Al} + \text{Mg} + \text{Fe})$ ratio of the PCA 91082 matrix is probably due to a lower abundance of smectite in it.

3.6. Phyllosilicate clasts

There are some phyllosilicate clasts in PCA 91082 that are different from dark inclusions (*e.g.* WEISBERG *et al.*, 1993; BISCHOFF *et al.*, 1993; ENDREß *et al.*, 1994). These phyllosilicate clasts are composed mainly of phyllosilicates with small amounts of fine-grained (sub- μm in size) opaque minerals and fine-grained (<3 μm) anhydrous minerals. Figure 1k is a BEI photograph of a phyllosilicate clast. It is composed of relatively large phyllosilicates with its interstices filled by finer phyllosilicates (Fig. 1l).

Chemical compositions of the phyllosilicate clast in Fig. 1l plotted on a $(\text{Si} + \text{Al})$ -Mg-Fe diagram (Fig. 7a) suggest that it is composed mainly of phyllosilicates with a very small amount of olivine. The $(\text{Si} + \text{Al})$ -Mg-Fe and $(\text{Mg} + \text{Fe})$ -Al-Si diagrams (Fig. 7) show that the phyllosilicates in the clast are the mixtures of serpentine and smectite. The phyllosilicates in the clast have similar compositions to the phyllosilicates in the Orgueil CI chondrite (TOMEOKA and BUSECK, 1988). The

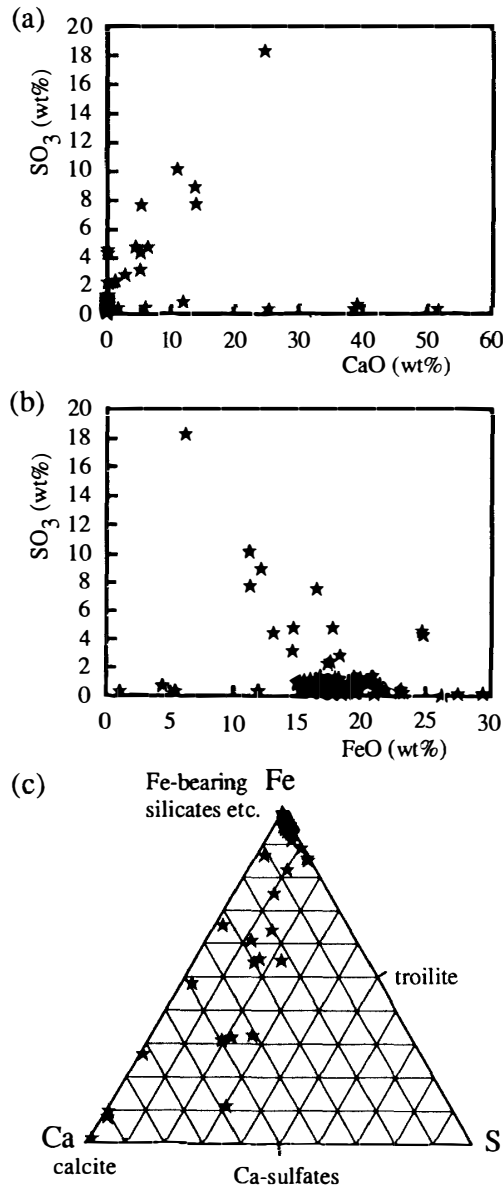


Fig. 11. Relationships between (a) CaO and SO_3 , (b) FeO and SO_3 , and (c) Fe, Ca, and S atomic % in a phyllosilicate clast in PCA 91082. In a plot of CaO vs. SO_3 (Fig. 11a), most of the analyses of the phyllosilicate clasts are plotted near the origin and correspond to phyllosilicates. In the figure, there are two trends. The first one is plotted along the CaO axis. The second trend shows a positive correlation between CaO and SO_3 wt% . Analyses which form the second trend have a negative correlation between FeO and SO_3 contents (Fig. 11b). These two plots indicate that the high SO_3 contents in some analyses do not result from the higher abundance of Fe-bearing sulfides (or sulfates) but a component which includes both Ca and S. The materials which are responsible for the Ca and S enrichment are probably Ca-sulfate(s). Although the atomic ratio between Ca and S of gypsum and anhydrite is unity, the ratio suggested from spot analyses of the phyllosilicate clast is higher than unity (Fig. 11c). Therefore, a Ca-carbonate component may be associated with a Ca-sulfate component.

phyllosilicates in Orgueil are composed of saponite and serpentine (TOMEOKA and BUSECK, 1988).

The CaO wt% of the phyllosilicate clast shows an interesting correlation with the SO_3 wt% (Fig. 11). In a plot of CaO vs. SO_3 (Fig. 11a), most of the analyses of the phyllosilicate clasts are plotted near the origin and correspond to the phyllosilicates. In the figure, there are two trends. The first one is along the CaO axis. In the second trend, there is a positive correlation between CaO and SO_3 wt% . Analyses which form the second trend have a negative correlation between FeO and SO_3 contents (Fig. 11b). These two plots indicate that the high SO_3 contents in some analyses do not result from the higher abundance of Fe-bearing sulfides (or sulfates) but a component which includes both Ca and S. Intensity maps of Ca, S, and Fe K_{α} lines show that where both Ca and S concentrate, Fe is depleted (Fig. 9d-f). Ca and S enriched areas appear sporadically in the clast. The largest Ca and S enriched area is

indicated by arrows in Fig. 11. The shapes and occurrences of the Ca and S enriched areas suggest that they are perhaps heavily altered Ca-rich pyroxene rims on low-Ca pyroxene. The materials which are responsible for the Ca and S enrichment are probably Ca-sulfate(s). The atomic ratio between Ca and S of gypsum and anhydrite is unity. However, the ratio suggested from spot analyses of the phyllosilicate clast is higher than unity (Fig. 11c). Therefore, a Ca-carbonate component may be associated with a Ca-sulfate component.

4. Bulk Compositions of Components in PCA 91082

Bulk compositions of refractory-rich inclusions, chondrules, and the matrix of PCA 91082 are plotted on (Si+Al)-Mg-Fe and (Mg+Fe)-Al-Si, and Al-Na-Ca diagrams (Fig. 12). Major element compositions of these components in PCA 91082 (Fig. 12a and b) are similar to those in the CV3 chondrites belonging to the reduced group (McSWEEN, 1977), such as Efremovka (*e.g.* NOGUCHI, 1994). As described in

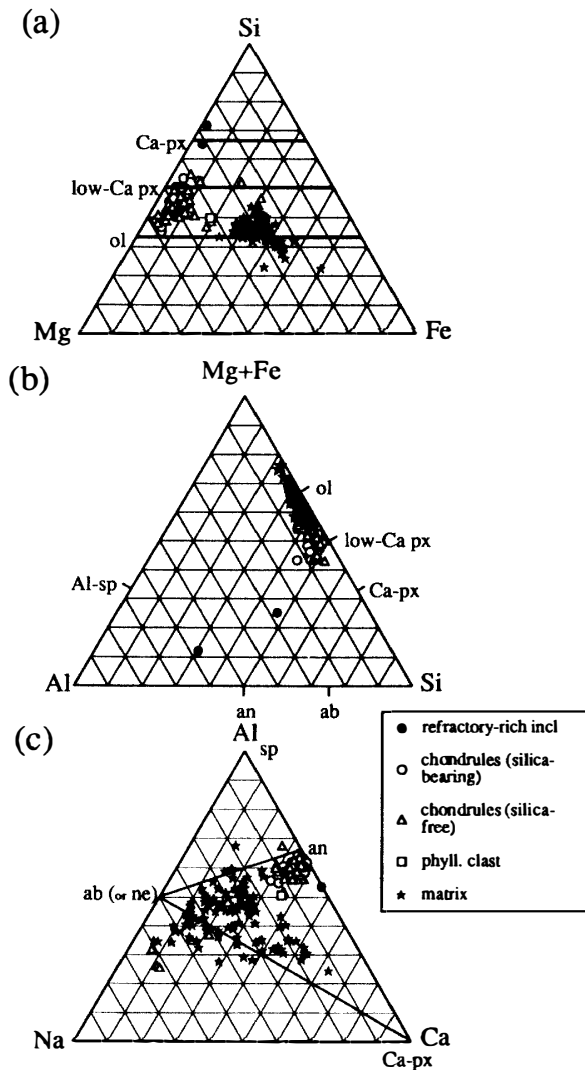


Fig. 12. Bulk compositions of refractory-rich inclusions, chondrules, a phyllosilicate clast, and the matrix in PCA 91082. These diagrams are plotted based on the atomic ratios in this paper. Major element compositions of these components in PCA 91082 are similar to those in the CV3 chondrites belonging to the reduced group (McSWEEN, 1977), such as Efremovka (*e.g.* NOGUCHI, 1994). Because the extent of aqueous alteration shown in PCA 91082 chondrules is low, the bulk compositions of chondrules in this meteorite were probably not changed greatly by the aqueous alteration processes. Analyses of the matrix are fairly homogeneous on the Si-Mg-Fe diagram (Fig. 12a). Because the bulk composition of the matrix was analyzed by defocused beams (20 μm in diameter), the proportions of constituent minerals of the matrix are homogeneous on a scale of 20 μm . The $\text{Na}/(\text{Al}+\text{Na}+\text{Ca})$ ratios of most of the matrix analyses are higher than those in refractory-rich inclusions, the phyllosilicate clast, and most of the chondrules (Fig. 12c). $\text{Na}/(\text{Al}+\text{Na}+\text{Ca})$ ratios of some chondrules are as high as those of the matrix. They are type II chondrules. Abbreviations: ol, olivine; low-Ca px, low-Ca pyroxene; Ca-px, Ca-pyroxene; an, anorthite; ab, albite; ne, nepheline; Al-sp, aluminous spinel.

the previous section, parts of chondrules are replaced by Fe-rich phyllosilicates. However, the extent of aqueous alteration shown in chondrules is low. Therefore, the bulk compositions of chondrules in this meteorite were probably not changed greatly by the aqueous alteration processes. Bulk compositions of silica-bearing chondrules overlap those of silica-free chondrules. Analyses of the matrix are fairly homogeneous on the Si-Mg-Fe diagram (Fig. 12a). Because bulk composition of the matrix was analyzed by defocused beams (20 μm in diameter), proportions of constituent minerals of the matrix are homogeneous on a scale of 20 μm . In Fig. 12c, chondrules are plotted near the anorthite component. The $\text{Na}/(\text{Al}+\text{Na}+\text{Ca})$ ratios of most of the matrix analyses are higher than those in refractory-rich inclusions, one phyllosilicate clast, and most of the chondrules (Fig. 12c). $\text{Na}/(\text{Al}+\text{Na}+\text{Ca})$ ratios of some chondrules are as high as those of the matrix. They are type II chondrules.

5. Discussion

5.1. Formation of silica-bearing chondrules in PCA 91082

As described in Section 3.3, many type I chondrules in PCA 91082 contain silica pods. Silica pods are observed in the outermost parts of the chondrules. Silica is associated with low FeO crystalline phases (low-Ca pyroxene, Ca pyroxene, and plagioclase), glass and phyllosilicates. At least four mechanisms to form these silica-bearing chondrules can be considered. They are (1) crystallization from SiO_2 -rich chondrule melts, (2) fractional crystallization of chondrules, (3) reduction of the outermost parts of chondrules, and (4) accretion of silica-rich materials on chondrules.

Bulk compositions of chondrules in this meteorite are not especially SiO_2 -rich, although SiO_2 -rich chondrules are more common in this meteorite than in the CV3 chondrites (Fig. 12a). Therefore, in contrast to the case of silica-bearing chondrules in Murchison CM2 chondrites, the first mechanism is ruled out.

If the fractional crystallization of chondrules had been the mechanism to form silica-bearing chondrules, residual chondrule melts must have been efficiently segregated into the peripheries of the chondrules. To segregate residual melts and then to form compositional zoning of chondrule glass, a special cooling history is needed. In the earlier stage of chondrule crystallization, relatively rapid growth of olivine must have occurred, following by slow crystallization of olivine and low-Ca pyroxene in the later stage to form porphyritic texture. Bulk compositional ranges of both silica-bearing and silica-free chondrules overlap each other (Fig. 10). Compositional zoning of chondrule glass within each chondrule was observed in both kinds of chondrules. Compositions of minerals in both kinds of chondrules cannot be distinguished from each other. Therefore, it is difficult to form the silica-bearing chondrules only by fractional crystallization. Furthermore, if such a special cooling history had occurred, chemical compositions in olivine and pyroxene in chondrules in PCA 91082 would have been different from those in the other CR chondrites because these minerals contained minor elements in higher amounts during rapid growth. However, there is no difference between chemical compositions of these minerals in PCA 91082 and those in the others. Therefore, the second mechanism is not plausible.

To explain the positive correlation between Ni and Co contents in Fe-Ni metal in chondrules, the reduction of chondrules has been proposed (LEE *et al.*, 1992; ZANDA *et al.*, 1993). However, compositions of ferromagnesian silicates seem not to support the reduction process. WEISBERG *et al.* (1993) reported that the Cr₂O₃ and FeO contents of olivine in the chondrule margins are slightly higher (up to 0.7 and 1.4 wt%, respectively) than those in the chondrule cores, and that TiO₂, Al₂O₃, and FeO contents of low-Ca pyroxene in the margins are slightly lower (up to 0.1, 0.9, and 0.6, respectively) than those in the cores. In PCA 91082, compositions of olivine and low-Ca pyroxene in the chondrule margins overlap those in the chondrule cores. Even if olivine and pyroxene in the rims were to be FeO-free by the reduction process, it seems to be difficult to enrich enough SiO₂ to crystallize the silica phase in chondrule melts, because FeO contents in olivine and pyroxene are, at best, a few wt%. Moreover, it is difficult to increase Na and K, and decrease Ca in chondrule glass in the chondrule rims only by reduction. Therefore, the third mechanism is ruled out.

If silica-rich materials had accreted on some chondrules, such materials would have been formed somewhere in the nebula. Such materials contain more SiO₂, Na₂O, and K₂O, and less Al₂O₃ and CaO. If the accretion of silica-rich materials on chondrules had occurred, it must have occurred when chondrules were partially molten, because there is no textural sharp boundary between silica-bearing chondrule rims and chondrule cores. Gradual changes of Na₂O, K₂O, and CaO contents were probably accomplished by diffusion during the cooling stage of chondrules. The outline of the multilayered type I chondrules in this meteorite is sinuous (Fig. 1c). Silica was often observed in the swells of the sinuous chondrule margins. One silica-bearing microchondrule (50×100 μm) whose mineralogy is the same as that in the margins of silica-bearing chondrules was found. These data may support the idea of adhesion of silica-rich material. In contrast to the case of ordinary chondrites, fayalite-silica assemblage was not observed in this meteorite. Therefore, two mechanisms can be thought to form silica-rich materials: gas-solid separation before the complete condensation of Si (*e.g.* BRIGHAM *et al.*, 1986) and disequilibrium condensation (*e.g.* WASSON and KROT, 1994).

In CR chondrites, oxygen isotopic compositions of bulk chondrites and constituent components plot on a mixing line with an inclination of 0.7 (WEISBERG and PRINZ, 1991a, b; WEISBERG *et al.*, 1993). Chondrule margins have heavier oxygen isotopic compositions than their coexisting cores even in the case of almost unaltered chondrules (WEISBERG *et al.*, 1992). The data can be interpreted by adhesive growth of chondrule precursor materials with different oxygen isotopic compositions on molten chondrules or unequilibrated oxygen isotopic exchange between chondrules and ambient gas. As a result, adhesion of silica-rich materials on chondrules is the most plausible mechanism. In this case, the adhered materials must have had different oxygen isotopic compositions, or an oxygen isotopic exchange reaction must have occurred.

5.2. Comparison of chemical composition of phyllosilicates in chondrules and matrices in PCA 91082 and Y-793495

Because there are abundant unaltered chondrules, the extent of aqueous alteration of chondrules is low (*e.g.* WEISBERG *et al.*, 1993; BISCHOFF *et al.*, 1993) in

both PCA 91082 and Y-793495. Only chondrule margins are altered in them. Major element compositions of the chondrule phyllosilicates in PCA 91082 are similar to those in Y-793495 although the $Fe/(Si+Al+Mg+Fe)$ ratios of the chondrule phyllosilicates in PCA 91082 tend to be higher than those in Y-793495 (Figs. 7a and 13a). Figure 13 suggests that some exceptional data in Fig. 13a are probably due to relict chondrule glass, plagioclase, pyroxene, and Fe-bearing phase(s). Figure 13 suggests that the chondrule phyllosilicates in Y-793495 are the mixtures of smectite, Al-rich serpentine (or chlorite), and serpentine. The $Fe/(Si+Al+Mg+Fe)$ ratios of matrix in Y-793495 are lower than those in the chondrule phyllosilicates (Figs. 14a

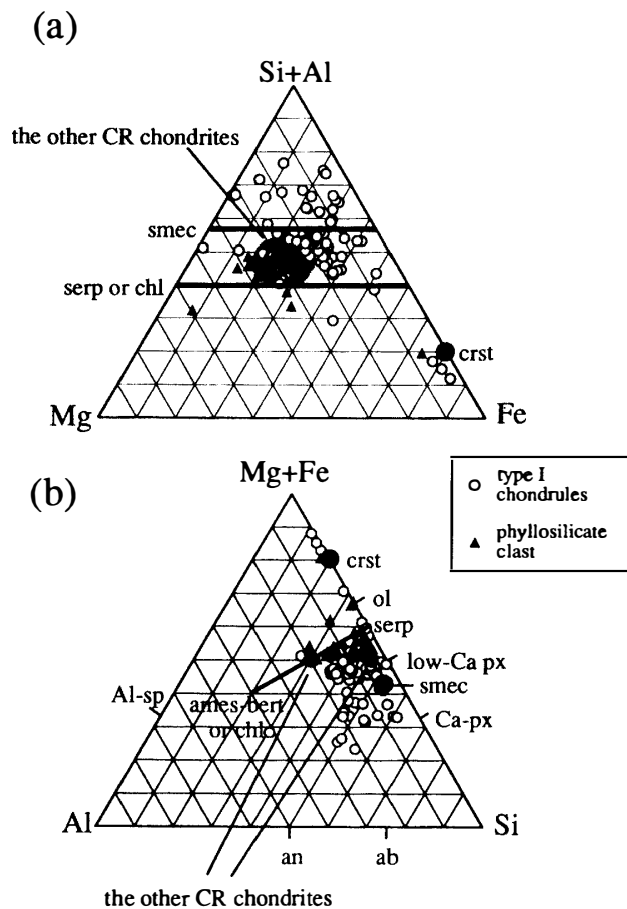


Fig. 13. Chemical compositions of phyllosilicates in chondrules and a phyllosilicate clast in Y-793495. (a) A $(Si+Al)$ - Mg - Fe diagram. (b) A $(Mg+Fe)$ - Al - Si diagram. Compositions of phyllosilicates in the other CR chondrites (WEISBERG et al., 1993) and compositions of some minerals are also indicated. These diagrams are plotted based on atomic ratios in this paper. Major element compositions of the chondrule phyllosilicates in PCA 91082 are similar to those in Y-793495 although the $Fe/(Si+Al+Mg+Fe)$ ratios of the chondrule phyllosilicates in PCA 91082 tend to be higher than those in Y-793495 (Figs. 7a and 13a). Some exceptional data in Fig. 13a are probably due to relict chondrule glass, pyroxene, and the Fe-bearing phase(s). The chondrule phyllosilicates in Y-793495 are the mixtures of saponite, Al-rich serpentine (or chlorite), and serpentine. Abbreviations are the same as those in Fig. 7.

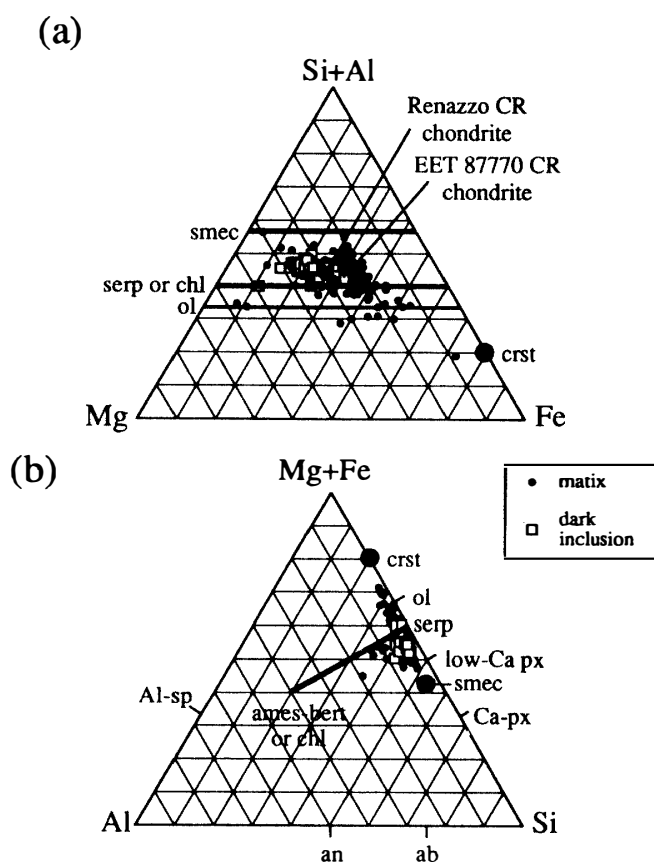


Fig. 14. Chemical compositions of the matrix in Y-793495. (a) A (Si+Al)-Mg-Fe diagram. (b) A (Mg+Fe)-Al-Si diagram. Compositions of the matrix average compositions in Renazzo and EET 87770 (ZOLENSKY et al., 1993) and those of some minerals are also indicated. This figure suggests that the matrix of Y-793495 is the mixtures of saponite, serpentine, and olivine. Abbreviations are the same as those in Fig. 7.

and 13a). This tendency is common to the case of PCA 91082 (Figs. 7a and 10a). Figure 14 suggests that the matrix of Y-793495 is the mixtures of saponite, serpentine, and olivine. In Figs. 13 and 14, compositions of a phyllosilicate clast and a dark inclusion are also indicated. The dark inclusion in Y-793495 is the mixtures of serpentine and smectite with a small amount of Al-rich serpentine or chlorite and relic olivine. The phyllosilicate clast in Y-793495 is the mixtures of Al-rich serpentine (or chlorite), serpentine, and saponite. In contrast to the case of the phyllosilicate clast in PCA 91082, most spot analyses of the phyllosilicate clast in Y-793495 exceed 90 total wt%. Therefore, it is suggested that it also contains abundant relic olivine. The Fe/(Si+Mg+Fe) ratios of the phyllosilicate clast are at the lowest end of the range of the ratio in matrix and similar to those in a dark inclusion.

The (Si+Al)-Mg-Fe diagrams show that the Fe/(Fe+Mg) ratios decrease in the following order: phyllosilicates in chondrules, matrices, and phyllosilicate clasts in both meteorites (Figs. 7, 10, 13, and 14). The extent of aqueous alteration in Renazzo and Al Rais chondrules is higher than that in PCA 91082 and Y-793495. The Fe contents in the phyllosilicates in chondrules in these less altered CR chondrites are higher than those in the more altered CR chondrites. However, more investigation is

needed to demonstrate the idea that Fe contents in phyllosilicates decreased as aqueous alteration proceeded because compositions of chondrule phyllosilicates in Renazzo do not differ from that in Al Rais although these meteorites experienced different degrees of aqueous alteration (WEISBERG *et al.*, 1993).

Irrespective of type I or II chondrules, unaltered and weakly altered chondrule glass in PCA 91082 contains more SiO_2 and less Al_2O_3 than those in Y-793495. $\text{Na}_2\text{O}+\text{K}_2\text{O}$ contents in the glass in PCA 91082 are also richer than those in Y-793495 (Fig. 15). Crystallization of silica in PCA 91082 chondrules is probably related to these compositional differences. It is remarkable that some analyses of unaltered and weakly altered chondrule glass in PCA 91082 show high K_2O concentrations (up to 3 wt%). Such chondrule glass is observed only in the chondrule margins. Na_2O and K_2O concentrations in phyllosilicates in PCA 91082 are higher than those in Y-793495. Average Na_2O and K_2O contents in phyllosilicates in PCA 91082 are 1.15 and 0.26 wt%. Those in Y-793495 are 0.35 and 0.16 wt%. There is a positive correlation between Al_2O_3 and $\text{Na}_2\text{O}+\text{K}_2\text{O}$ in phyllosilicates in chondrules in Y-793495 (Fig. 15b). However, there is no correlation (or weak negative correlation) between them in PCA 91082 (Fig. 15a). $\text{Na}_2\text{O}+\text{K}_2\text{O}$ concentrations in the matrix in PCA 91082 are higher than those in Y-793495 as is the case of the phyllosilicates in chondrules. Na_2O and K_2O contents in the matrix are lower than those in the phyllosilicates in both PCA 91082 and Y-793495 (0.82 and 0.11 wt% in PCA 91082; 0.32 and 0.10 wt% in Y-793495). Because the alkaline elements to Al atomic ratios in phyllosilicates do not exceed 1, there is no phyllosilicate which is plotted near the ordinate in Fig. 15. The CI-normalized abundance of Na in CR chondrites varies

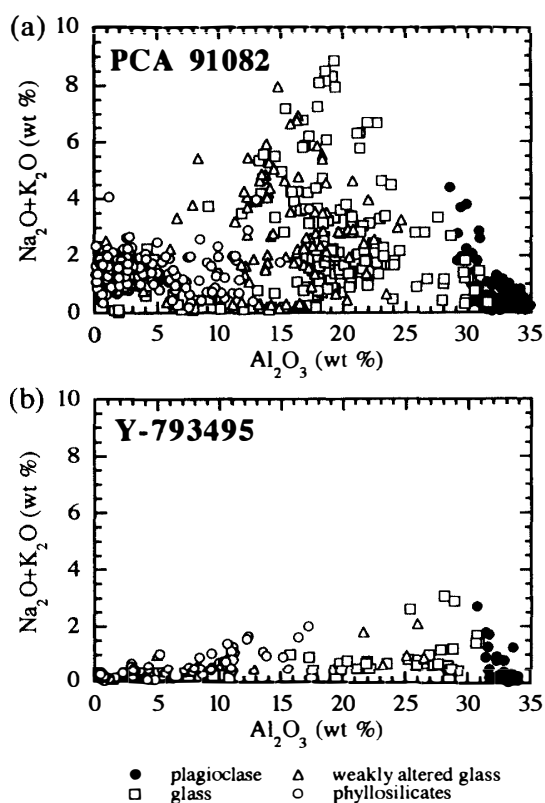


Fig. 15. Relationships between Al_2O_3 and $\text{Na}_2\text{O}+\text{K}_2\text{O}$ in plagioclase, chondrule glass, weakly altered chondrule glass, and phyllosilicates in magnesian chondrules in (a) PCA 91082 and (b) Y-793495. $\text{Na}_2\text{O}+\text{K}_2\text{O}$ contents in chondrule glass in PCA 91082 are higher than those in Y-793495. Crystallization of silica in PCA 91082 is probably related to these compositional differences. There is a positive correlation between Al_2O_3 and $\text{Na}_2\text{O}+\text{K}_2\text{O}$ in phyllosilicates in chondrules in Y-793495. However, there is no correlation (or there is a weak negative correlation) between them in PCA 91082.

among chondrites (KALLEMEYN *et al.*, 1994). The abundance in Renazzo is about 0.45. The values in PCA 91082, Y-793495, and heavily weathered Acfer 059 are about 0.35, about 0.18, and 0.15. There is a possibility that compositions of phyllosilicates in chondrules and the matrix in Y-793495 may be slightly modified by terrestrial weathering.

5.3. *A phyllosilicate clast in PCA 91082 and its implication for the aqueous alteration condition*

As described in Section 3.6, a phyllosilicate clast contains a Ca-sulfate component with magnesian phyllosilicates. The possibility of the presence of a Ca-sulfate component is important in considering the aqueous alteration conditions of this meteorite. Before we go further, we have to consider the possibility of Ca-sulfate as a terrestrial weathering product. However, the possibility is probably low, because the coexisting phases and the occurrences of Ca-sulfates (*e.g.* gypsum) formed by terrestrial weathering are different from those observed in this meteorite. GOODING (1986) shows that gypsum coexists with clay mineraloids, K-Fe-sulfates [jarosite: $\text{KFe}^{3+}_3(\text{SO}_4)_2(\text{OH})_6$], cryptocrystalline rust, zeolites, and secondary alkaline feldspar in terrestrial weathering products in Antarctic meteorites.

The terrestrial weathering products occur as fracture filling materials of fusion crusts, or decomposition products of glass and plagioclase in interior samples of achondrites (GOODING, 1986). However, in this case, the appearance of a Ca-sulfate component is restricted to a specific area in the phyllosilicate clast as shown in Figs. 1i and 9a–c and in a specific dark inclusion. The texture of the clast suggests that it is a heavily altered chondrule. Because alteration in most of the chondrules is low, heavy alteration shown in the clast does not result from terrestrial weathering. The area where the Ca-sulfate component is concentrated on was probably a Ca-pyroxene rim around a low-Ca pyroxene phenocryst. If so, the texture suggests that Ca-pyroxene was replaced by a Ca-sulfate component and phyllosilicates by the aqueous alteration.

This study shows that there is a compositional difference between the phyllosilicate clast and the matrix. Phyllosilicates in the phyllosilicate clast are more magnesian than the host matrix. Phyllosilicates in heavily altered CM chondrites and some heavily altered carbonaceous chondrites like Y-86720 are more magnesian than those in weakly altered CM chondrites (*e.g.* ZOLENSKY *et al.*, 1993). This compositional difference results from the participation of magnesian olivine and pyroxene in aqueous the alteration process. Therefore, the texture and composition of the phyllosilicate clast suggest that some phyllosilicate clasts in PCA 91082 seem to have been chondrules which suffered severe aqueous alteration. After aqueous alteration, constituent components which experienced different degrees of aqueous alteration were agglomerated. This interpretation is plausible because CR chondrites are breccias (*e.g.* WEISBERG *et al.*, 1993; BISCHOFF *et al.*, 1993).

Phyllosilicates in a phyllosilicate clast in PCA 91082 have similar composition to those in CI chondrites and are associated with a Ca-sulfate component. CI chondrites contain Ca-sulfate. It is thought that Ca- and Mg-sulfates in CIs were formed during aqueous alteration on a CI parent body. (*e.g.* RICHARDSON, 1978; FREDRIKSSON and KERRIDGE, 1988). Ca-sulfates in CI chondrites occurs in veins. The occurrence is different from that in this clast. The different occurrences of Ca-sulfates between this

clast and CI chondrites were perhaps due to different permeabilities of starting materials. Probably the phyllosilicate clast in PCA 91082 also suffered aqueous alteration on a meteorite parent body. According to ZOLENSKY *et al.* (1989, 1993), the temperature (50–150°C) and water/rock ratio of aqueous alteration of CI and CR are similar, but fO_2 of aqueous alteration of CI reaches a higher level than that of CR. However, because the phyllosilicate clast in PCA 91082 contains a Ca-sulfate component and contains only a small amount of Fe-sulfide component, this clast probably experienced aqueous alteration under higher fO_2 and lower fS_2 conditions, like CI chondrites. The data perhaps suggest that the CR parent body was layered or that there was more than one parent body which experienced different degrees of aqueous alteration.

6. Conclusions

1) PCA 91082 contains abundant chondrules as described by MASON (1993). This meteorite contains small amounts of refractory-rich inclusions.

2) Chemical compositions of low-Ca pyroxene, olivine, and Fe-Ni metal in PCA 91082 are within the range of the CR chondrites which were investigated by WEISBERG *et al.* (1993).

3) Chondrules in PCA 91082 contain abundant glass in their interior. Only the chondrule margins show alteration. Phyllosilicates in chondrules are Fe-rich and Al-poor. Fe contents in the phyllosilicates in chondrules are higher than the values reported in other CR chondrites. Ca-carbonates were not observed in the rims of chondrules in PCA 91082.

4) About 40% of investigated chondrules in PCA 91082 contain silica in their outermost parts. Silica was probably formed by the adhesion of SiO_2 -rich materials during chondrule formation.

5) Compositions of phyllosilicates in chondrules and matrices in PCA 91082 and Y-793495 are different from each other. The compositional differences would be due to the difference of starting materials (mainly compositions of chondrule glass), the extent of aqueous alteration and perhaps terrestrial weathering.

6) A phyllosilicate clast in PCA 91082 contains a Ca-sulfate component with magnesian phyllosilicates. Probably it experienced aqueous alteration on a parent body. The aqueous alteration condition of the phyllosilicate clast was probably similar to that of CIs. PCA 91082 contains constituent components which experienced various alteration conditions.

Acknowledgments

I am grateful to the Meteorite Working Group of NASA and Drs. K. YANAI and H. KOJIMA of the National Institute of Polar Research for giving the loan of the meteorite thin sections. Drs. M. KIMURA and M. K. WEISBERG are thanked for their helpful discussion and comments. Drs. M. K. WEISBERG and T. NAKAMURA are appreciated for their reading the manuscript and giving detailed comments. The manuscript was greatly improved by their comments. Scanning electron microscopy

and computer-aided compositional mapping analysis were performed at the Geological Institute, University of Tokyo. Mr. H. YOSHIDA and Mrs. H. WADA are gratefully acknowledged for providing technical support when I performed scanning electron microscopy and computer-aided compositional mapping. This work was supported by the Grant-in-Aid for Scientific Research, from the Ministry of Education, Science and Culture, Japan (No. 05740332).

References

- AKAI, J. and KANNO, J. (1986): Mineralogical study of matrix- and groundmass-phyllosilicates, and isolated olivines in Yamato-791198 and -793321: With special reference to new finding of 14 Å chlorite in groundmass. *Mem. Natl Inst. Polar Res., Spec. Issue*, **41**, 259–275.
- BARBER, D. J., MARTIN, P. M. and HUTCHEON, I. D. (1984): The microstructure of minerals in coarse-grained Ca-Al-rich inclusions from the Allende meteorite. *Geochim. Cosmochim. Acta*, **48**, 769–783.
- BENCE, A. E. and ABLEE, A. L. (1968): Empirical correction factors for the electron microanalysis of silicates and oxides. *J. Geol.*, **76**, 382–403.
- BISCHOFF, A., PALME, H., ASH, R. D., CLAYTON, R. N., SCHULTZ, L. *et al.* (1993): Paired Renazzo-type (CR) carbonaceous chondrites from the Sahara. *Geochim. Cosmochim. Acta*, **57**, 1587–1603.
- BRIGHAM, C. A., YABUKI, H., OUYANG, Z., MURRELL, M. T., EL GORESY, A. and BURNETT, D. S. (1986): Silica-bearing chondrules and clasts in ordinary chondrites. *Geochim. Cosmochim. Acta*, **50**, 1655–1666.
- ENDREB, M., KEIL, K. and BISCHOFF, A. (1992): Dark clasts in the Acfer 059/El Djouf 001 meteorite (CR) from the Sahara: Implications for their origin. *Meteoritics*, **27**, 218–219.
- ENDREB, M., KEIL, K., BISCHOFF, A., SPETTEL, B., CLAYTON, R. N. and MAYEDA, T. K. (1994): Origin of dark clasts in the Acfer 059/El Djouf 001 CR2 chondrites. *Meteoritics*, **29**, 26–40.
- FREDRIKSSON, K. and KERRIDGE, J. F. (1988): Carbonates and sulfates in CI chondrites: Formation by aqueous activity on the parent body. *Meteoritics*, **23**, 35–44.
- GOODING, J. L. (1986): Clay-mineraloid weathering products in Antarctic meteorites. *Geochim. Cosmochim. Acta*, **50**, 2215–2223.
- GROSSMAN, J. N., RUBIN, A. E., NAGAHARA, H. and KING, E. A. (1988): Properties of chondrules. *Chondrites and the Early Solar System*, ed. by J. F. KERRIDGE and M. S. MATTHEWS. Tucson, Univ. Arizona Press, 436–461.
- GROSSMAN, L. and OLSEN, E. (1974): Origin of the high temperature fraction of C2 chondrites. *Geochim. Cosmochim. Acta*, **38**, 173–187.
- KALLEMEYN, G. W., RUBIN, A. and WASSON, J. T. (1994): The compositional classification of chondrites: VI. The CR carbonaceous chondrite group. *Geochim. Cosmochim. Acta*, **58**, 2873–2888.
- LEE, M. S., RUBIN, A. E. and WASSON, J. T. (1992): Origin of metallic Fe-Ni Renazzo and related chondrites. *Geochim. Cosmochim. Acta*, **56**, 2521–2533.
- MASON, B. (1993): Antarctic Meteorite Newsletter, **16**, 22.
- MACPHERSON, G. J. and GROSSMAN, L. (1984): “Fluffy” type A Ca-, Al-rich inclusions in the Allende meteorite. *Geochim. Cosmochim. Acta*, **48**, 29–46.
- MACPHERSON, G. J., WARK, D. A. and ARMSTRONG, J. T. (1988): Primitive material surviving in chondrites: Refractory inclusions. *Chondrites and the Early Solar System*, ed. by J. F. KERRIDGE and M. S. MATTHEWS. Tucson, Univ. Arizona Press, 746–807.
- McSWEEN, H. Y. (1977): Petrographic variations among carbonaceous chondrites of the Vigarano type. *Geochim. Cosmochim. Acta.*, **41**, 1777–1790.
- McSWEEN, H. Y. (1979): Are carbonaceous chondrites primitive or processed? A review. *Rev. Geophys. Space Phys.*, **17**, 1059–1078.
- NOGUCHI, T. (1989): Texture and chemical composition of pyroxenes in chondrules in carbonaceous and unequilibrated ordinary chondrites. *Proc. NIPR Symp. Antarct. Meteorites*, **2**, 204–233.
- NOGUCHI, T. (1994): Petrology and mineralogy of the Coolidge meteorite (CV4). *Proc. NIPR Symp.*

- Antarct. Meteorites, **7**, 204–233.
- NOGUCHI, T., FUJINO, K. and MOMOI, H. (1993): Phyllosilicates in chondrules and matrix in the Murchison chondrite. Papers presented to the 18th NIPR Symposium on Antarctic Meteorites, May 31–June 2, 1993. Tokyo, National Inst. Polar Res., 100–104.
- OLSEN, E. J. (1983): SiO₂-bearing chondrules in the Murchison (C2) meteorite. Chondrules and Their Origins, ed. by E. A. KING. Houston, Lunar Planet. Inst., 235–242.
- RICHARDSON, S. M. (1978): Vein formation in the C1 carbonaceous chondrites. Meteoritics, **13**, 141–159.
- SHENG, Y. J., HUTCHEON, D. and WASSERBURG, G. J. (1991): Origin of plagioclase-olivine inclusions in carbonaceous chondrites. Geochim. Cosmochim. Acta, **55**, 581–599.
- TOMEOKA, K. and BUSECK, P. (1988): Matrix mineralogy of the Orgueil CI carbonaceous chondrite. Geochim. Cosmochim. Acta, **52**, 1627–1640.
- WARK, D. A. (1987): Plagioclase-rich inclusions in carbonaceous chondrite meteorites: Liquid condensates? Geochim. Cosmochim. Acta, **51**, 221–242.
- WASSON, J. T. and KROT, A. N. (1994): Fayalite-silica association in unequilibrated ordinary chondrites: Evidence for aqueous alteration on a parent body. Earth Planet. Sci. Lett., **122**, 403–416.
- WEBER, D. and BISCHOFF, A. (1992): Mineralogy and chemistry of refractory inclusions in CR-like chondrites from the Sahara desert. Lunar and Planetary Science XXIII. Houston, Lunar Planet Inst., 1505–1506.
- WEISBERG, M. K. and PRINZ, M. (1990): Refractory-rich inclusions in CR2 (Renazzo-type) chondrites. Lunar and Planetary Science XXI. Houston, Lunar Planet Inst., 1315–1316.
- WEISBERG, M. K. and PRINZ, M. (1991a): Aqueous alteration in CR2 chondrites. Lunar and Planetary Science XXII. Houston, Lunar Planet Inst., 1483–1484.
- WEISBERG, M. K. and PRINZ, M. (1991b): El Djouf 001: A new CR chondrite. Meteoritics, **26**, 1406–407.
- WEISBERG, M. K., PRINZ, M. and NEHRU, C. E. (1988): Petrology of ALH 85085: a chondrite with unique characteristics. Earth Planet. Sci. Lett., **91**, 19–32.
- WEISBERG, M. K., PRINZ, M., CLAYTON, R. N. and MAYEDA, T. K. (1992): Formation of layered chondrules in CR2 chondrites: A petrologic and oxygen isotopic study. Meteoritics, **27**, 306.
- WEISBERG, M. K., PRINZ, M., CLAYTON, R. N. and MAYEDA, T. K. (1993): The CR (Renazzo-type) carbonaceous group and its implications. Geochim. Cosmochim. Acta, **57**, 1567–1586.
- ZANDA, B., HEWINS, R. H. and BOURROT-DENISE, M. (1993): Metal precursors and reduction in Renazzo chondrules. Meteoritics, **28**, 466–467.
- ZOLENSKY, M. (1991): Mineralogy and matrix composition of “CR” chondrites Renazzo and EET 87770, and ungrouped chondrites Essebi and MAC 87300. Meteoritics, **26**, 414.
- ZOLENSKY, M., BARRETT, R. and BROWNING, L. (1993): Mineralogy and composition of matrix and chondrule rims in carbonaceous chondrites. Geochim. Cosmochim. Acta, **57**, 3123–3148.
- ZOLENSKY, M., BOURCIER, W. L. and GOODING, J. L. (1989): Aqueous alteration on the hydrous asteroids: Results of EQ3/6 computer simulations. Icarus, **78**, 411–425.

(Received August 12, 1994; Revised manuscript received December 7, 1994)